

## RESEARCH ARTICLE

10.1002/2015WR018525

# Time-varying nonstationary multivariate risk analysis using a dynamic Bayesian copula

Ali Sarhadi<sup>1</sup>, Donald H. Burn<sup>1</sup>, María Concepción Ausín<sup>2</sup>, and Michael P. Wiper<sup>2</sup>

<sup>1</sup>Department of Civil and Environmental Engineering, University of Waterloo, Waterloo, Ontario, Canada, <sup>2</sup>Departamento de Estadística, Universidad Carlos III de Madrid, Getafe, Spain

### Key Points:

- A multivariate nonstationary risk framework is proposed by developing a dynamic copula
- A fully time-varying joint return period concept is developed for multivariate risk analysis
- The nature and risk of multidimensional processes are changed over time under climate change

### Supporting Information:

- Supporting Information S1
- Movie S1

### Correspondence to:

A. Sarhadi,  
asarhadi@uwaterloo.ca

### Citation:

Sarhadi, A., D. H. Burn, M. C. Ausín, and M. P. Wiper (2016), Time-varying nonstationary multivariate risk analysis using a dynamic Bayesian copula, *Water Resour. Res.*, 52, 2327–2349, doi:10.1002/2015WR018525.

Received 17 DEC 2015

Accepted 1 MAR 2016

Accepted article online 4 MAR 2016

Published online 30 MAR 2016

**Abstract** A time-varying risk analysis is proposed for an adaptive design framework in nonstationary conditions arising from climate change. A Bayesian, dynamic conditional copula is developed for modeling the time-varying dependence structure between mixed continuous and discrete multiattributes of multidimensional hydrometeorological phenomena. Joint Bayesian inference is carried out to fit the marginals and copula in an illustrative example using an adaptive, Gibbs Markov Chain Monte Carlo (MCMC) sampler. Posterior mean estimates and credible intervals are provided for the model parameters and the Deviance Information Criterion (DIC) is used to select the model that best captures different forms of nonstationarity over time. This study also introduces a fully Bayesian, time-varying joint return period for multivariate time-dependent risk analysis in nonstationary environments. The results demonstrate that the nature and the risk of extreme-climate multidimensional processes are changed over time under the impact of climate change, and accordingly the long-term decision making strategies should be updated based on the anomalies of the nonstationary environment.

## 1. Introduction

Global warming is a major threat to the planet. This warming is a result of an increase in human-induced greenhouse gas emissions and is altering Earth's climate. According to the Intergovernmental Panel on Climate Change (IPCC), changes in characteristics of the water cycle due to rising temperatures have hydrological implications [IPCC, 2014; Milly *et al.*, 2015]. Thus, global warming will impact hydrological processes and lead to increased risk of climate extremes in different parts of the world.

Water professionals struggle to develop approaches that account for the impact of climate change on hydrological designs to reduce associated risks. Traditional, risk-based decision-making principles in water resources planning are based on the fundamental assumption of statistical stationarity. Under stationarity, it is assumed that the probabilistic characteristics of hydrometeorological processes will not change over time, and that future water resources planning can be designed with past records in mind. Milly *et al.* [2008, 2015] argued that the fundamental assumption of stationarity has been influenced by climate change and anthropogenic effects, and therefore it is no longer applicable for water resources risk assessment and planning. Accordingly, water planners must revise current planning and analytic strategies to develop nonstationary probabilistic models based on the anomalies of the changing environment arising from climate change [Read and Vogel, 2015; Salas and Obeysekera, 2013]. Therefore, in the changing environment an effective and flexible time-varying design approach must be adopted for risk-based decision-making in water resources planning and infrastructure designs.

Under nonstationary conditions, the behavior of extreme hydrometeorological processes changes and their probabilistic parameters may no longer be constant. Vogel *et al.* [2011] introduced a "flood magnification factor" to quantify how the distribution of extreme events shifts from decade to decade under the impact of a broad range of anthropogenic activities, including climate change. In this condition, alternative approaches should be developed in which the effect of nonstationarity is integrated and probabilistic parameters are allowed to change over time. In this case, statistical distribution parameters are expressed as functions of covariates to model the changing conditions associated with nonstationarity generated by climate change impacts. A covariate could take the form of a time-dependent trend in the moments of hydro-meteorological variable time series or low-frequency climatological signals [Du *et al.*, 2015; Katz *et al.*, 2002].

Univariate nonstationarity modeling in hydrological risk assessment has drawn a great deal of attention in hydrological science in recent years [Rosner *et al.*, 2014; Salas and Obeysekera, 2013; Westra *et al.*, 2014]. Khaliq *et al.* [2006] reviewed approaches used for the nonstationary frequency analysis of hydrometeorological variables. Bayesian approaches have gained more attention for nonstationary modeling in recent years. Studies that use Bayesian techniques for the analysis of hydrometeorological variables, include Cunderlik *et al.* [2007], Ouarda and El-Adlouni [2011], El Adlouni and Ouarda [2009] for at-site frequency analysis, and Khaliq *et al.* [2006] and Leclerc and Ouarda [2007] for regional frequency analysis at ungauged areas. These studies were carried out under nonstationary conditions in a univariate context, while it is well known that natural stochastic hydrometeorological processes are multivariate phenomena by their very nature characterized by multiattribute properties that are statistically dependent. Accordingly, univariate risk analysis methods under nonstationarity conditions cannot fully characterize the properties that are highly correlated. This inability may lead to high uncertainty and failure of risk plans in water resources systems. For a complete understanding of multivariate hydrometeorological extreme events under the impact of climate change, it is therefore necessary to study the simultaneous, multivariate, probabilistic behavior of two or more hydrological properties. Since being introduced and applied in hydrology and geosciences by De Michele and Salvadori [2003], the application of copulas in modeling the dependence behavior of hydrological processes has grown quickly in recent years [Chebana and Ouarda, 2011; Hao and Singh, 2012; Lee *et al.*, 2013; Madadgar and Moradkhani, 2013, 2014; Requena *et al.*, 2013; Sadri and Burn, 2012; Santhosh and Srinivas, 2013]. However, these studies and similar ones have not taken into account the effects of nonstationarity and assumed a constant dependence relation over time, which is not appropriate under changing environment. Wahl *et al.* [2015] also demonstrated increasing risk of compound flooding through exhibiting nonstationarity in the dependence between two natural hazards, heavy precipitation, and storm surge, at major U.S. coastal cities. Using the lowest and highest values of dependency separately, they attempted to show changes on joint return periods relevant to flood risk analyses at the beginning and the end of a time period, ignoring time-varying nonstationarity in a multivariate risk analysis.

Multivariate, nonstationary risk analysis is relatively new and very few publications are available in the literature regarding this area. Chebana *et al.* [2013] first mentioned the idea of using multivariate functions with changing dependence structure between multivariate hydrological attributes over time. Corbella and Stretch [2013] also applied conditional copula functions with invariant dependence metrics. Despite their importance, dependence structures affected by the changing environments between different individual hydrological attributes have scarcely been investigated. Bender *et al.* [2014] presented a bivariate nonstationary approach to study the time-dependent behavior of bivariate hydrological design parameters. Jiang *et al.* [2015] also performed a bivariate frequency analysis with time variation in dependence structure for the low-flow series from two hydrological neighbor stations. Nevertheless, practical mathematical issues arise when dealing with time-varying dependence of two or more attributes over time in multivariate nonstationary stochastic modeling. For example existing studies only use simple, linear trend estimators to model the distribution function parameters. The methods are not fully time-varying in terms of functions, especially in definition of return period concept. Furthermore, they are not assessing time-varying risk concept for an adaptive multivariate design framework over future long-time periods. Thus, few theoretical hydrological studies on the concept of time-varying multivariate nonstationary modeling exist. This is partly related to the unavailability of robust methods and the complexity of parameter estimation techniques.

While frequentist methods have been preferred for estimating distribution parameters, Bayesian inference offers more attractive framework in terms of time-varying copula estimation [Smith, 2013]. In particular, Bayesian inference for dynamic copulas has been studied in the financial context by Ausin and Lopes [2010] and Creal and Tsay [2015]. However, to the authors' best knowledge, no study is available in the literature that discusses adapting Bayesian inference for multivariate conditional dynamic copula modeling in the water resource management area. Thus, this insight is new in hydrology and should prompt a strong interest in multivariate copula-based models with time-varying dependence parameters under nonstationary conditions. To promote a robust methodology to deal with the concept, the present study proposes a time-varying copula capturing the time evolution in the changing dependence structures under multimodel ensembles of climate change scenarios. Full likelihood-based Bayesian inference is developed where the whole set of the model parameters are estimated in an adaptive multivariate time-varying design framework. The proposed methodology is employed on the complex natural phenomenon, drought, which

stands first among all others affecting the most people [Tallaksen and van Lanen, 2004], as an illustrative case study.

This paper is organized as follows: section 2 describes the main properties of drought process that is used as an illustrative case study and the climate data set used in this study. Section 3 presents the mathematical background of the Bayesian dynamic copula model used to assess time-varying risk in an adaptive nonstationary water-planning framework under changing climate conditions. The results and discussion of the case study follow in the section 4, and finally the conclusions and potential future works for wider applications are drawn.

## 2. Illustrative Study and Data Set

### 2.1. Definition of Drought Characteristics

Drought is a complex natural hazard. Some reasons arise from the dynamic complexity of droughts. Others are caused by lack of knowledge about this natural hazard. Some aspects of these reasons can be summarized in several ways. First, drought is recognized as a creeping process whose impacts start slowly and then accumulate over a considerable period of time and may linger for a long time after the termination of the drought event. Second, there is no precise and universal definition for drought, which makes it difficult to deal with such a phenomenon [Mishra and Singh, 2010]. Third, the impacts of drought result in nonstructural damages spreading over a large geographical area varying in spatial and temporal scales [Mishra and Singh, 2010; Wilhite, 2000]. Unlike some other natural hazards, humans can directly trigger drought and aggravate it through impacting land's capacity for receiving and holding water [Mishra and Singh, 2010]. The other way that humans affect drought is by the indirect impact of climate change, which is created by global warming from greenhouse gas emissions. This process can adversely exacerbate drought characteristics.

Droughts are dynamic and multiattribute in nature. One cannot assess and describe them by characterizing a single feature for any type of analysis. There is a need to find an appropriate way to define different properties of drought using underlying indices. A list of the most prominent indices, which have been widely used to define different types of droughts, is found in Mishra and Singh [2010]. One of these, formed by monthly time series of precipitation—Standardized Precipitation Index (SPI)—and developed by McKee *et al.* [1993], is used to represent multivariate drought characteristics under the run theory context. SPI's simplicity, its spatial invariance in its interpretation, its probabilistic nature, and its presentation of better spatial standardization with respect to extreme events, have made it a powerful and specialized indicator for precise quantification of drought [Lloyd-Hughes and Saunders, 2002; Mishra and Singh, 2010]. The fundamental superiority of SPI relative to other drought indices is that it can be calculated for a variety of time scales. This flexibility enables SPI to monitor precipitation anomalies on short-term and long-term water supplies from soil moisture to streamflow, groundwater, and reservoir storage supplies [Mishra and Singh, 2010]. This index is calculated by fitting a Gamma distribution to the monthly precipitation data. The Gamma cumulative distribution function (CDF) is then rescaled so that an index of SPI = 0 is the median precipitation. This index applies to different time scales ranging from 1 to 24 months. A drought period is assumed as a consecutive number of time intervals when SPI values are less than the truncation level (SPI = 0). Therefore, drought duration is defined as the number of consecutive events with negative-SPI, while drought severity is the cumulative value of the negative-SPI within the drought duration as given in the following form [Mishra and Singh, 2011; Shiau, 2006]:

$$S = - \sum_{i=1}^D \text{SPI}_i \tag{1}$$

where  $S$  denotes drought severity, and  $D$  denotes drought duration. In this case, severity attribute is a continuous measurement and is described as "continuous random variable," while duration attribute values are discretized and rounded to integer numbers and can assume finite or countably infinite number of values. Thus, duration attribute is considered a "discrete random variable."

As a dynamic and alternating process, drought occurrences take into account interarrival time expression for the recurrence interval of droughts. Interarrival time denoted as  $X$  is thus defined as the period elapsing

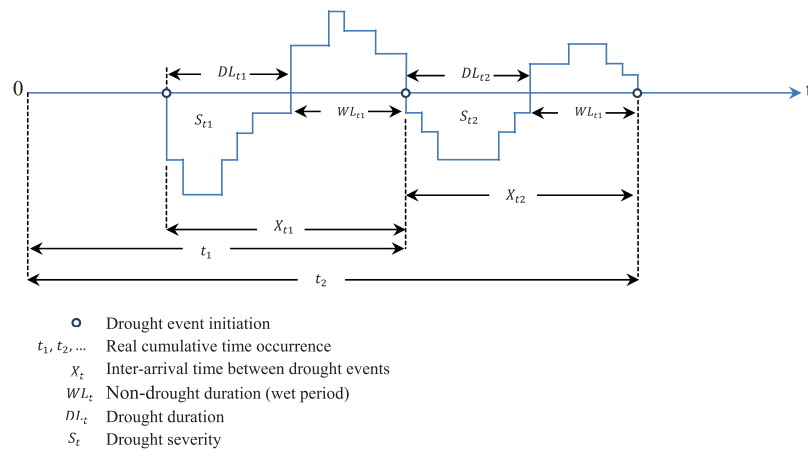


Figure 1. Dynamic drought renewal process and definition of drought characteristics in a changing environment.

from the initiation of a drought event to the beginning of the next event [Song and Singh, 2010]. Similar to duration attribute, the discretized interarrival time attribute is also described as “discrete random variable.” The probabilistic characteristics of the defined drought attributes may be influenced due to natural internal climate processes or external forcing as a consequence of human influences. In the changing nonstationary environment, each of the attributes may change over time. Figure 1 shows the alternating process and time-varying characteristics of droughts defined by the given concept over time.

To implement the adaptive time-varying nonstationary multivariate risk framework, the capital of Iran, Tehran, is selected as the domain for the present study. A meteorological station in this megacity is selected as the study site to characterize the drought attributes. Figure 2 depicts the location of the study site. The management of surface water resources has been a main challenge for water authorities in Tehran in recent years with respect to rapid expansion of population and occurrence of severe long-term dry spells arising from climate change. It

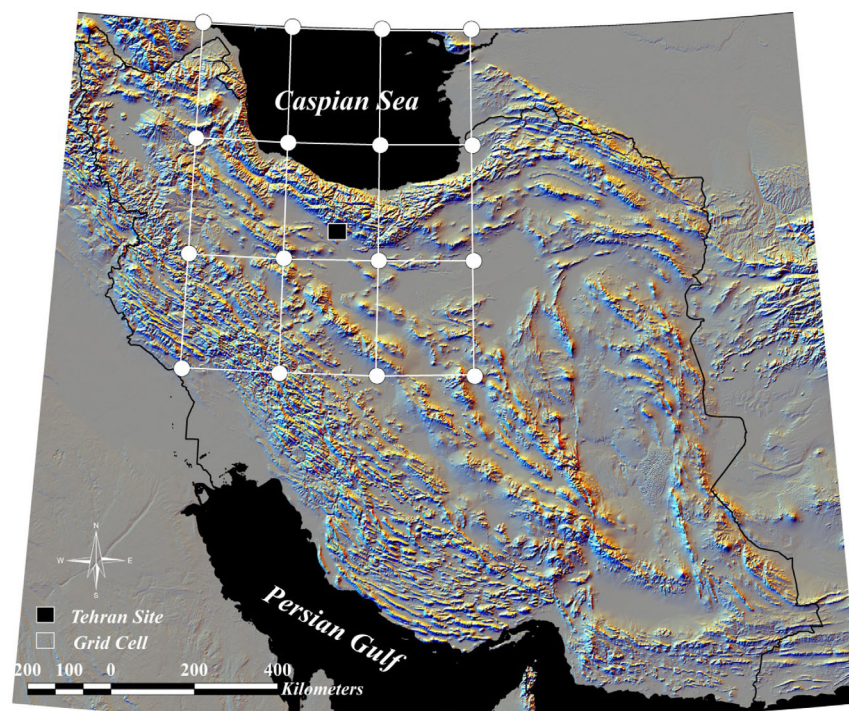


Figure 2. Study site and surrounding grid cells used in the statistical downscaling process.

is therefore of crucial importance to have a long-term management plan including the impact of climate change on the occurrence of dry spells and availability of surface water resources in this megacity.

Future precipitation (as predictand variable) in the study site is projected through a regression-based statistical downscaling process using nonlinear and soft computing techniques. In this procedure, reanalysis NCEP/NCAR data (extracted from nine grid cells surrounding the study site) are employed as a proxy of observed large-scale atmospheric predictors. Fifteen GCMs of the most recent CMIP5 multimodel ensemble, conducted in support of the Intergovernmental Panel on Climate Change (IPCC) Fifth Assessment Report (AR5) are used for simulation of atmospheric projectors. All the GCMs are regridded by bilinear interpolation method to match the resolution of the NCEP/NCAR reanalysis data  $2.5^\circ \times 2.5^\circ$ . A Multivariate Recursive Nesting Bias Correction (MRNBC) method is employed to correct the spatial and temporal biases on future simulation of atmospheric projectors. In the regression-based statistical framework, historical NCEP/NCAR reanalysis data-based atmospheric projectors are dimensionality reduced into a sequence of principal components having maximal dependency with the predictand variable (precipitation) using a nonlinear kernelized version of Supervised PCA. A fully probabilistic Bayesian model known as Relevance Vector Machine (RVM) is engaged to capture the nonlinear relationships between the predictand and dimension-reduced atmospheric predictors. The developed model is then applied on the future biased corrected and dimension-reduced large-scale atmospheric projectors from 15 GCMs to project the impact of climate change on the precipitation behavior under three different scenarios. The CMIP5 provides future simulations of atmospheric projectors with specified concentrations referred to as “representative concentration pathways” (RCPs), which are forced by anthropogenic influences on the atmospheric composition and land cover. The CMIP5 projections of future climate change underlying the RCPs provide a consistent combination of future population growth, technological advances, and socioeconomic parameters [Taylor *et al.*, 2012]. Three considered radiative forcing scenarios in the present study are RCP2.6, in which the radiative forcing is estimated to increase to about  $3 \text{ W/m}^2$  by year 2100 and decline afterwards, and also  $4.5 \text{ W/m}^2$  and  $8.5 \text{ W/m}^2$  in the other two scenarios, RCP4.5 and RCP8.5, respectively [Scoccimarro *et al.*, 2013; Taylor *et al.*, 2012]. More information about the downscaling procedure and the scenarios is given in Sarhadi *et al.* [2015].

To develop a risk-based water resources plan in a nonstationary condition, the limitations of the relatively short historical hydrometeorological records, and the uncertainties associated with future climate model projections, are considered major restrictions. To address these limitations, a time-varying stochastic model can be developed by synthesizing historical observed records and climate model projections using multiple climate forcing scenarios [Borgomeo *et al.*, 2014; Milly *et al.*, 2008]. Although the uncertainty of future projections is still problematic in a changing climate, using climate multimodel ensembles allows to quantify probabilistic uncertainties of hydrological processes in future climate projections. Hence, despite having inherent uncertainties, probabilistic information from multiple-model ensembles under different forcing scenarios helps to identify sources of uncertainty and to measure the influence degree of extreme events [Bayazit, 2015; Galloway, 2011]. To quantify future extreme dry spells in an adaptive time-varying design framework, based on the concept of design's life period [Rootzén and Katz, 2013], the relatively short historical precipitation time series (1951–2014) are synthesized with projected precipitation from multimodel ensemble GCMs (spanning from 2015 to 2100). Synthesizing probabilistic precipitation projections under different forcing scenarios (representing uncertainty of future precipitation behavior) with observed precipitation also helps experts better communicate the certainty of an event occurrence. In this way, assuming that probabilistic projections are reliable, decision makers are able to effectively manage the risk of the event occurring [DeChant and Moradkhani, 2015]. To develop a risk-based time-varying framework and to include all the possibilities and avoid additional calculations, one appropriate representative synthesized precipitation time series is selected from each climate change scenario. By making a boxplot of all the synthesized precipitation time series from all ensemble models in the different scenarios, one is able to select two models covering the minimum and the maximum variance of all the synthesized GCM models. In this way, all the possibilities (other models) are located in between these two selected models covering the whole variance of data. Doing so, synthesized MIRO-ESM CHEM model is selected from the scenario RCP2.6, and synthesized INMCM4 model is selected from the scenario RCP8.5, representing minimum and maximum variances of the all models, respectively. From the midrange mitigation emission scenario (RCP4.5) synthesized model of CanESM2 is also selected as the representative of this scenario class.

Choosing one representative model from each climate change scenario, the synthesized precipitation time series are used for forming SPI3 (SPI index for 3 month precipitation time series) to define the drought characteristics over the design's life period.

### 3. Methodology

#### 3.1. Time-Varying Multivariate Nonstationary Risk Analysis

Introduced by *Sklar* [1959], copulas are considered flexible tools for constructing multivariate distributions and modeling the dependence structure between correlated variables. The popularity of copulas is due to their flexibility in forming dependence between variables using any type of marginals. In addition, copulas are able to capture wide variety of dependence structures, including asymmetry, nonlinear, and tail dependence [*Jammazi et al.*, 2015]. More-detailed information about the properties of copulas is given in *Nelsen* [2007] and *Salvadori et al.* [2007].

Realizing a changing environment, a time-varying or dynamic conditional copula should be taken into account for water resources risk-based decision-making. Introduced by *Patton* [2006], in a financial framework, a dynamic copula allows a time variant dependence structure to characterize the relationship of underlying variables in a more flexible and time-varying manner. Suppose that  $\mathbf{y}_t = (y_{1t}, y_{2t})$  represents a pair of hydrological variables whose dependence structure is defined by a copula function. A general form of a time-varying joint distribution can be built at any time  $t$  using a dynamic copula as follows:

$$\begin{aligned} \mathbf{y}_t &\sim F(\mathbf{y}_t|\theta_t) \\ F(\mathbf{y}_t|\theta_t) &= C(F_1(y_{1t}|\theta_{1t}), F_2(y_{2t}|\theta_{2t})|\theta_{ct}) \\ F(\mathbf{y}_t|\theta_t) &= C(u_{1t}, u_{2t}|\theta_{ct}) \end{aligned} \quad (2)$$

where  $F(\cdot)$  denotes cumulative distribution function,  $C(\cdot)$  is the copula function,  $\theta_{1t}$  and  $\theta_{2t}$  are parameters for the time-varying marginal models,  $\theta_{ct}$  is the time-varying copula parameter, and  $u_{1t}$  and  $u_{2t}$  are marginal probabilities in the dynamic copula in the unit hypercube with uniform  $U[0, 1]$  marginal distributions.

In a multivariate, risk analysis framework, nonstationarity could be identified in the statistical characteristics of either one or two marginal variables and not in the dependence structure or vice versa. It might also happen that both the marginals and the dependence structure show nonstationary behavior. Nonstationarity can be via a trend component (i.e., linear or nonlinear) and (or) sudden changes in statistical attributes of the variables. The presence of trend or change point may have a considerable effect on the interpretation of results in fitting different probability distributions [*Khaliq et al.*, 2006]. To capture the possible nonstationarity of the marginals and the dependence in fitting probability distributions, various time-dependent approaches are employed in the context of univariate and multivariate nonstationary frequency analysis [*AghaKouchak et al.*, 2012; *Khaliq et al.*, 2006]. Local likelihood-based methods have gained more popularity and proven to be useful explanatory tools. These methods can be developed to include covariates to estimate distribution and copula parameters such that they vary over time. Various techniques have been utilized for this purpose, including the full maximum likelihood (FML) estimation, the canonical maximum likelihood (CML) method, inference functions for marginals (IFM) approach, and empirical copulas [*El Adlouni et al.*, 2007; *Jammazi et al.*, 2015; *Ouarda and El-Adlouni*, 2011].

In this study, marginal distribution parameters are specified as functions of time, which is viewed as a covariate, and are estimated via the generalized linear model approach capturing linear or nonlinear trends. Different forms of nonstationarity (sudden jump, periodicity, and trend) on the synthesized long-term drought observations are detected using classical statistical techniques such as nonparametric, univariate, and multivariate Mann-Kendall tests [*Chebana et al.*, 2013] on both the marginals and the dependence functions. The null hypothesis of no trend is rejected if the trend test statistic is different from zero at 5% significance level. In the following, the parameter estimation methods of the marginal distributions in the presence of the nonstationarities are discussed for each drought attribute.

##### 3.1.1. Time-Varying Marginal Distributions

As in the illustrative example of this study, two correlated drought attributes are different in terms of probabilistic behavior; different classes of independent distributions are used to construct their marginal distributions. In a nonstationary process, the parameters of the underlying marginal distributions are time-dependent, and hence, the stochastic behavior of these distributions varies over time [*Cheng and AghaKouchak*, 2014]. Upon detection of a significant trend, to capture the nonstationarity behavior, in this study, different forms of linear and nonlinear functions of time are discussed with respect to location parameter ( $\mu_t$ ) of the different marginal distributions. Other distribution parameters are kept constant in this case, although they could be similarly assumed to be time-varying. This leads to estimating drought quantiles in a more realistic way consistent with the behavior of observed and projected extreme drought

events [Cheng and AghaKouchak, 2014]. In the following, different forms of trend in regard with the time-dependent distribution parameters are discussed for the two drought attributes.

**3.1.1.1. Drought Severity Models**

As drought severity is considered a continuous random attribute, the most popular and well-fitted distributions in respect to this variable are Gamma and Log-Normal distributions [Janga Reddy and Ganguli, 2012; Shiau, 2006]. Let  $S_t$  be the severity attribute starting at (real) time  $t$ . Then the two proposed time-varying model possibilities will be as follows:

Log-Normal severity model:

$$\log S_t | \mu_t, \sigma \sim N(\mu_t, \sigma^2) \tag{3}$$

Gamma severity model:

$$S_t | \mu_t, \phi \sim Ga(\mu_t \phi, \phi) \tag{4}$$

with density function given by,

$$f(s_t | \mu_t, \phi) = \frac{\phi^{\mu_t \phi - 1}}{\Gamma(\mu_t \phi)} s_t^{\mu_t \phi - 1} \exp(-\phi s_t), \quad s_t > 0$$

with  $E[S_t] = \mu_t$ . In both models, the location parameter ( $\mu_t$ ) is assumed to be a function of time. Then, we consider different forms of constant, linear, and quadratic models for the location parameter as follows:

$$\begin{aligned} \mu_t &= \delta \\ \mu_t &= \delta + \epsilon t \\ \mu_t &= \delta + \epsilon t + \zeta t^2 \end{aligned} \tag{5}$$

where  $t$  is time. A similar structure can also be used in the case of the Gamma distribution such that, here we assume (for the quadratic model),

$$\log \mu_t = \delta + \epsilon t + \zeta t^2$$

Therefore, the set of severity model parameters is given by  $\beta_s = (\delta, \epsilon, \zeta, \sigma)$  if a Log-Normal model is chosen or, alternatively, by  $\beta_s = (\delta, \epsilon, \zeta, \phi)$  if a Gamma model is selected.

**3.1.1.2. Drought Duration Models**

According to the run-theory definition, droughts last as integer numbers of months, and drought duration is thus considered as a "discrete random variable." The majority of studies in multivariate frequency area have assumed drought duration as a continuous random variable. For example, Madadgar and Moradkhani [2013], Shiau [2006], Shiau and Modarres [2009], Halwatura et al. [2015], and other associated studies have fitted continuous probability distributions to discrete drought duration values. Other studies such as De Michele et al. [2013] suggested using a randomization technique known as "jittering" to transform discrete drought duration attribute to a continuous variable.

In this study, however, drought duration attribute is considered as a "discrete random variable" and "discrete distributions" are fitted to the drought duration time series. Assume droughts last an integer number of months,  $d \in \{1, 2, \dots\}$ , and that in a changing environment, as time goes on, drought durations and their variability may be increasing or decreasing. In this condition, we consider a time-varying duration model.

Let  $D_t$  be the duration of a drought, which starts at (real) time  $t$ . Then one possibility could be a Negative Binomial duration model:

$$\begin{aligned} \text{Let } Z_t &= D_t - 1 \\ \text{Then } Z_t | r, p_t &\sim NB(r, p_t) \\ \text{where } p_t &= r / (r + \lambda_t) \end{aligned} \tag{6}$$

with probability mass function given by,

$$\Pr(Z_t = z | r, p_t) = \binom{z+r-1}{z} p_t^r (1-p_t)^z, \quad z=0, 1, 2, \dots$$

Note that the Negative Binomial model generally allows for capturing overdispersed data. An alternative model could also be a Poisson duration model:

$$Z_t | \lambda_t \sim P_o(\lambda_t) \tag{7}$$

with probability mass function:

$$\Pr(Z_t = z | \lambda_t) = \frac{\lambda_t^z e^{-\lambda_t}}{z!}, \quad z=0, 1, 2, \dots$$

This model could be sometimes overly restrictive when there are many zeros in observations.

Another possible model for duration data is a Geometric distribution. This model corresponds to a particular case of the Negative Binomial model with  $r$  set to 1 although it is restricted to data that show strictly decreasing probabilities for higher durations.

In a changing climate, the rate of drought occurrence ( $\lambda_t$ ) is assumed to be time-dependent and varies over time. Similar to severity, different log trend forms, including constant, linear, and quadratic models can be employed for  $\lambda_t$  as follows:

$$\begin{aligned} \log \lambda_t &= \eta \\ \log \lambda_t &= \eta + \theta t \\ \log \lambda_t &= \eta + \theta t + \kappa t^2 \end{aligned} \tag{8}$$

where  $t$  is time and the set of duration model parameters is given by  $\beta_D = (\eta, \theta, \kappa, r)$ .

### 3.1.2. Dynamic Copula

To model the dependence between severity and duration attributes under a changing nonstationary condition, a dynamic copula needs to be developed. In the static states, and even in the existing time-varying studies, copula models have mostly been employed to construct dependence structure between only continuous random variables. In performing statistical inference for copula models in water resource risk studies, it happens some of marginals are discrete and the others are continuous, such as the illustrative example (drought). To our best knowledge, no studies exist in this area to consider the application of a dynamic copula for mixed attributes (discrete and continuous). By extending the classical copula model, one is able to develop a dynamic copula so that its parameter varies over time. This study presents an original approach, which can handle realistic, dynamic copula modeling in the case of mixed outcomes.

Let  $C_t(u_t, v_t)$  represent the dependence structure between severity and duration for a drought that begins at (real) time  $t$ , where  $u_t = F_{S_t}(s_t)$  and  $v_t = F_{D_t}(d_t)$  are the cumulative distribution functions of the severity and duration, respectively, at time  $t$ . In the current study, a time-varying Gumbel copula  $C(u_t, v_t | \theta_{ct})$  is developed for drought observations, as this exhibits greater dependence in the positive tail than in the negative and is therefore one of the possible copula functions for extreme value analyses [AghaKouchak et al., 2012; Chebana and Ouarda, 2011]. The time-varying distribution function of a Gumbel copula is given by:

$$C(u_t, v_t | \theta_{ct}) = \exp \left\{ - \left[ (-\log u_t)^{\theta_{ct}} + (-\log v_t)^{\theta_{ct}} \right]^{\frac{1}{\theta_{ct}}} \right\} \tag{9}$$

where  $\theta_{ct} \in [1, \infty]$  and the density function is given by:

$$\begin{aligned} c(u_t, v_t | \theta_{ct}) &= C(u_t, v_t | \theta_{ct}) u_t^{-1} v_t^{-1} \left[ (-\log u_t)^{\theta_{ct}} + (-\log v_t)^{\theta_{ct}} \right]^{-2 + \frac{2}{\theta_{ct}}} \\ &\times \left[ (\log u_t)(\log v_t) \right]^{\theta_{ct} - 1} \left\{ 1 + (\theta_{ct} - 1) \left[ (-\log u_t)^{\theta_{ct}} + (-\log v_t)^{\theta_{ct}} \right]^{-\frac{1}{\theta_{ct}}} \right\} \end{aligned} \tag{10}$$

The relation between the dependence parameter of the Gumbel copula and the standard, Kendall's tau dependence values can be expressed as:

$$\tau_t = 1 - 1/\theta_{ct} \tag{11}$$

where the Gumbel copula parameter is defined for  $\tau_t$  in (0,1) so that there is positive dependence as reflected in the real drought observations.



To capture different forms of Kendall’s tau under changing nonstationary conditions, the following models are assumed:

$$\begin{aligned} \log \frac{\tau_t}{1-\tau_t} &= \zeta \\ \log \frac{\tau_t}{1-\tau_t} &= \zeta + vt \\ \log \frac{\tau_t}{1-\tau_t} &= \zeta + vt + \chi t^2 \end{aligned} \tag{12}$$

The copula parameter,  $\theta_{ct}$ , is thus defined as a deterministic function of time,  $t$ , and a vector of unknown parameters,  $\beta_C = (\zeta, v, \chi)$ .

Following the same concept, other members of the Archimedean or elliptical families of copulas could also be considered.

### 3.1.3. Time-Varying Joint Return Period

In planning and management of water resources, risk assessment is a crucial task requiring estimation of the recurrence intervals of extreme events. Recurrence intervals of events are characterized by the concept of return periods in hydrology. In the multivariate domain, different transformation types of the joint exceedance probability to a joint return period (JRP) have been suggested in literature [Gräler et al., 2013; Salvadori et al., 2007; Shiau, 2006]. There is still discussion on which form of the JRP could be more appropriate in water resources planning and project design [Bender et al., 2014]. Following the method introduced by De Michele et al. [2013] and Gräler et al. [2013], in this study, a fully time-varying framework evolving through time is proposed for joint return period. We define the time-varying joint return period at time  $t$ , denoted by  $JRP_t(d_0, s_0)$ , as the expected time between droughts with duration larger than  $d_0$  and severity larger than  $s_0$  at time  $t$ :

$$JRP_t(d_0, s_0) = \frac{E[X_t]}{1 - F_{D_t}(d_0) - F_{S_t}(s_0) + P(D_t \leq d_0, S_t \leq s_0)} \tag{13}$$

where  $X_t$  is the mean interarrival time between drought events.

Since with the evolution of a drought, interarrival time between events may vary over time, the behavior of this variable may be time-dependent, this attribute can also be modeled through potential discrete probability distributions such as those fitted to drought duration in the previous section.

Let  $X_t$  be the interarrival time between drought events, which starts at (real) time  $t$ . Then similar to drought duration, one possible model could be a Negative Binomial interarrival model:

$$\begin{aligned} \text{Let } M_t &= X_t - 2 \\ \text{Then } M_t | s, q_t &\sim NB(s, q_t) \\ \text{where } q_t &= s / (s + \gamma_t) \end{aligned} \tag{14}$$

Other discrete distributions, including Poisson and Geometric can also be fitted. Similar to the drought duration, constant, linear, and quadratic models (shown in equation (8)) are also used to express the time-varying  $\gamma_t$ . In this case, a set of interarrival model parameters is given by  $\beta_A = (\psi, \omega, \vartheta)$ .

Taking into account the interarrival time as a time-varying variable, and given the time dependent marginal distributions for the duration and severity, the fully time-varying joint return period is given by:

$$JRP_t(d_0, s_0) = \frac{\gamma_t + 2}{1 - u_{t_0} - v_{t_0} + C(u_{t_0}, v_{t_0} | \theta_{ct})} \tag{15}$$

Observe that if we have nonstationary drought durations and severities, such that these increase with time, it is expected that the time-varying joint return period,  $JRP_t(d_0, s_0)$  will decrease as  $t$  increases for each pair of values,  $d_0, s_0$ . Therefore, the time-varying return period in a nonstationary condition depends on the time-varying parameters of the interarrival times, marginal distribution and dynamic copula. It should be noted that the other forms of the joint return period can also be developed using the same concept.

### 3.2. Bayesian Inference of Dynamic Copula

In a multivariate, nonstationary risk analysis framework under a nonstationary environment, uncertainty assessment of the dynamic copula using time as a covariate is of fundamental importance. In this study, a Bayesian Markov Chain Monte Carlo (MCMC) approach is integrated to the nonstationary marginal and copula models to characterize the uncertainty. In this approach, for all the time-varying variables (including marginals, interarrival-time, and copula) a Bayesian inference scheme is implemented to indirectly estimate the time-varying distribution parameters,  $\mu_t$ ,  $\lambda_t$ ,  $\theta_{ct}$ , and  $\gamma_t$ . For this purpose, instead of directly inferring these distribution parameters, Bayesian inferences are employed to estimate the generalized linear model parameters  $\beta_S$ ,  $\beta_D$ ,  $\beta_{A_t}$ , and  $\beta_{C_t}$  respectively, linking the parameter values at time  $t$  with the time as a covariate.

Bayesian inference defines prior distributions for all unknown generalized linear model parameters  $\beta_S$ ,  $\beta_D$ ,  $\beta_{A_t}$ , and  $\beta_{C_t}$ . Then, the knowledge brought by a prior distribution is combined with the given observations to generate posterior distribution by Bayes theorem. More specifically, we consider a two-step Bayesian approach where we first make inference for the marginal parameters of the drought severity,  $\beta_S$ , duration,  $\beta_D$  and interarrival time,  $\beta_{A_t}$ . Then, in the second step, we make inference for the copula parameters,  $\beta_{C_t}$ , given the results for the marginal parameters. Assume for example that we have a sample of severities,  $s_{t_1}, \dots, s_{t_n}$ , observed at  $n$  instant times,  $t_1, \dots, t_n$ . Suppose that we have considered a time-varying Gamma model for the severity as defined in (4). Then, the posterior distribution for the severity parameters  $\beta_S = (\partial, \varrho, \iota, \phi)$ , is given by,

$$p(\beta_S | s_{t_1}, \dots, s_{t_n}) \propto p(\beta_S) \prod_{i=1}^n p(s_{t_i} | \beta_S) \tag{16}$$

where  $p(\beta_S)$  is the prior density and

$$p(s_{t_i} | \beta_S) = \frac{\phi^{\mu_{t_i} \phi^{-1}}}{\Gamma(\mu_{t_i} \phi)} s_{t_i}^{\mu_{t_i} \phi^{-1}} \exp(-\phi s_{t_i}),$$

and where  $\log \mu_{t_i} = \partial + \varrho t_i + \iota t_i^2$ . Consequently, the generated posterior distribution,  $p(\beta_S | s_{t_1}, \dots, s_{t_n})$ , provides information on the posterior distribution of the time-varying parameter,  $\mu_t$ , for each time,  $t$ . Note that in the case of stationarity  $\varrho$  and  $\iota$  are equal to zero and the parameter  $\mu_t$  remains constant and consequently, the severity observations are independent and identically distributed.

#### 3.2.1. Prior Distributions

The prior distributions are used to provide any prior knowledge on the parameters,  $\beta_S$ ,  $\beta_D$ ,  $\beta_{A_t}$ , and  $\beta_{C_t}$ . Thus, prior distributions are independent from observations and are preferably specified using external source of knowledge [AghaKouchak et al., 2012]. In the current illustrative example, proper but weakly informative priors are assumed in the case of drought severity model as:

$$\begin{aligned} \partial &\sim N(0, 1000) \\ \varrho &\sim N(0, 1000) \\ \iota &\sim N(0, 1000) \end{aligned} \tag{17}$$

and  $\phi \sim \text{Ga}(0.01, 0.01)$ , if a Gamma model is considered for the severity distribution. In the case of the lognormal model,  $N(0,1000)$  prior distributions are also used for  $\delta$ ,  $\epsilon$ , and  $\zeta$  and  $\tau \sim \text{Ga}(0.01, 0.01)$  where  $\tau = \frac{1}{\sigma^2}$ .

Similarly, for the duration parameters,  $N(0, 1000)$  priors are set for  $\theta$ ,  $\kappa$  and a Gamma prior  $\text{Ga}(0.01, 0.01)$  is also used for  $r$ . Likewise, priors of the same form are used for the equivalent parameters of the interarrival time distribution.

For the copula parameters, it is assumed that  $\zeta \sim N(0, 1000)$  and very precise priors  $\nu \sim N(0, 1000)$ , as well as  $\chi \sim N(0, 10^{-9})$  to avoid numerical problems with the increase of  $t$ . Note that if good expert information were available, then they could be used to define more informative prior distributions.

#### 3.2.2. Bayesian MCMC Inference

In general for our models, analytic evaluation of the posterior distributions is not possible. To estimate parameters inferred by Bayes, an MCMC sampling method is integrated to generate an approximate Monte Carlo sample of realizations from the posterior distributions. While there are different types of MCMC sampling algorithms, the Gibbs sampler approach is employed in the current study to obtain samples from a

joint distribution through iterative sampling from the full conditional distributions. For example, in order to generate a sample from the joint posterior distribution (16) of the severity parameters, under a given model,  $\beta_S = (\delta, \epsilon, \zeta, \phi)$ , a systematic form of the Gibbs sampler algorithm proceeds as follows [Dellaportas and Smith, 1993]:

0. Set initial values  $\delta^{(0)}, \epsilon^{(0)}, \zeta^{(0)}, \phi^{(0)}$ .
1. Repeat for  $m=1, \dots, M$ .
2. Sample from  $p(\delta | \epsilon^{(m-1)}, \zeta^{(m-1)}, \phi^{(m-1)}, s_{t_1}, \dots, s_{t_n})$
3. Sample from  $p(\epsilon | \delta^{(m)}, \zeta^{(m-1)}, \phi^{(m-1)}, s_{t_1}, \dots, s_{t_n})$
4. Sample from  $p(\zeta | \delta^{(m)}, \epsilon^{(m)}, \phi^{(m-1)}, s_{t_1}, \dots, s_{t_n})$
5. Sample from  $p(\phi | \delta^{(m)}, \epsilon^{(m)}, \zeta^{(m)}, s_{t_1}, \dots, s_{t_n})$

Repeated iteration of the above procedure yields a sequence,  $\beta_S^{(m)} = (\delta^{(m)}, \epsilon^{(m)}, \zeta^{(m)}, \phi^{(m)})$ , which is a realization of the MCMC. To ensure the full convergence of the chains and also minimizing the influence of initialization, the so-called burn-in samples are discarded from the chain. The remaining samples are then used for inference. This procedure can be implemented using the free software WinBUGS (<http://www.mrc-bsu.cam.ac.uk/software/bugs/>), which is run via the R2WinBUGS interface in R software.

To assess the convergence of the Markov chain, a convergence diagnosis method proposed by Geweke [1991] is used. According to the Geweke test, if the convergence is achieved, the Geweke statistic will have an asymptotically standard Gaussian distribution. More information about this test is given in Geweke [1991]. Following the underlying MCMC Bayesian inference, the credibility intervals and the uncertainty of nonstationary probabilities of the generalized linear models' parameters can also be obtained.

### 3.2.3. Model Selection

To select the best proposed models, a Bayesian discrimination criterion is employed. The Deviance Information Criterion (DIC) defined by Spiegelhalter et al. [2002] is a measure specifically designed for model selection under Bayesian inference and can be thought of as a Bayesian alternative to the standard AIC. Once samples of the posterior distributions for the parameters of the different trend models (including, constant, linear, and quadratic) are obtained using Bayesian MCMC inference, the DIC measure can be easily calculated. For example, the DIC value for a severity model is obtained as [Spiegelhalter et al., 2002]:

$$DIC = D(\bar{\beta}_S) + 2n_D \tag{19}$$

where  $D(\beta_S)$  is the deviance:

$$D(\beta_S) = -2 \sum_{i=1}^n \log p(s_{t_i} | \beta_S)$$

and  $\bar{\beta}_S = E(\beta_S | s_{t_1}, \dots, s_{t_n})$ , is the posterior mean, which can be approximated from the MCMC output using,

$$\bar{\beta}_S \simeq \frac{1}{M-B} \sum_{m=1}^{M-B} \beta_S^{(m)},$$

where  $B$  is the number of burn-in iterations, and  $n_D$  is the effective number of parameters of the model which is given by:

$$n_D = \bar{D} - D(\bar{\beta}_S) \tag{20}$$

where  $\bar{D} = E(D(\beta_S) | s_{t_1}, \dots, s_{t_n})$  is the posterior deviance, which assesses the model's goodness of fit and can be approximated by,

$$\bar{D} \simeq \frac{1}{M-B} \sum_{m=1}^{M-B} D(\beta_S^{(m)}) \tag{21}$$

The DIC can be measured in a straightforward way from the WinBUGS output. Note that the minimum value of the DIC indicates the best model.

**Table 1.** Results of the Best Selected Distribution, and Univariate and Multivariate Mann-Kendall Trend Statistics for Each Drought Attribute in Different Scenarios

Scenario	Models	Attributes	Selected Dist.	Univariate MK	P value	Multivariate MK	P value
RCP2.6	MIRO-ESM CHEM	Severity	Gamma	0.67	0.49		
		Duration	Neg. Binomial	2.07	<b>0.04*</b>	-	-
		Copula	Gumbel			1.39	0.16
RCP4.5	CanESM2	Inter-arrival	Neg. Binomial	-1.54	0.12		
		Severity	Gamma	1.25	0.21		
		Duration	Neg. Binomial	2.39	<b>0.01*</b>		
RCP8.5	INMCM4	Copula	Gumbel			1.85	0.06
		Inter-arrival	Neg. Binomial	-2.35	<b>0.02*</b>		
		Severity	Gamma	1.86	<b>0.04*</b>		
		Duration	Neg. Binomial	2.47	<b>0.01*</b>		
		Copula	Gumbel			2.21	<b>0.02*</b>
		Inter-arrival	Neg. Binomial	-3.09	<b>0.001**</b>		

\*, 5% significance level; \*\*, 1% significance level.

## 4. Results and Discussion

### 4.1. Preprocessing Analyses

For selection of an appropriate model in frequency analysis process, the first step is to check if there is any non-stationarity in the data set. Prior to this step, based on nonparametric goodness-of-fit tests (Chi-square test for discrete drought attributes and Kolmogorov-Smirnov test for continuous one), the best distribution functions are fitted to the synthesized drought characteristics for the selected GCM models under different forcing climate change scenarios. Table 1 shows the best selected distribution for each attribute in different scenarios.

According to *Chebana et al.* [2013], it is recommended to jointly analyze univariate and multivariate trend tests to capture all existing trend components as the signs of nonstationarity. The output of the Mann-Kendall test in univariate and multivariate cases of the drought attributes in different models are shown in Table 1. It should be noted that the trend results are achieved after testing serial correlation and change point detection for univariate properties, and change point detection for multivariate copula attribute. The results indicate that in the low and midrange emission scenarios (RCP2.6 and RCP4.5) only duration attributes exhibit the presence of nonstationarity, whereas in a severe forcing scenario (RCP8.5) all the univariate and multivariate attributes of the selected synthesized model show significant trend. In the latter model, all severity, duration, and copula variables exhibit significant upward trend, while interarrival time attribute shows significant downward trend.

### 4.2. Estimation and Selection of Time-Varying Models Using MCMC Sampling

The distribution parameters of the marginals and copula are estimated through the posterior distribution of the MCMC samples. Considering a trend imposes a certain type of nonstationarity, outputs of posterior distributions should be actively checked to select the best statistical model capturing the nonstationarity form. Three different modes of the posterior distributions are employed in the parameter estimations to select the best fitted model. Mode 0 (M0) is used when nonstationary model does not fit to the model, indicating the mean parameter of distribution ( $\mu$ ) or dependence  $\theta_{ct}$  is time invariant. Mode 1 (M1) is accounted for a nonstationary condition by assuming the model parameter is a linear function of time. In mode 2 (M2), a quadratic function is used to model the nonstationarity in the distribution parameters and dependence structure. In all climate change scenarios, the Gibbs algorithm is used to generate independent Monte Carlo samples that are used for convergence diagnosis. In each case, the MCMC algorithm is run for 30,000 iterations, which are drawn from the posterior distribution. The first 3000 samples are discarded as burn-in and the rest are used for computing the parameter estimations. Having an asymptotically standard normal distribution, the results of the Geweke's statistic, (with absolute values less than 1.96) indicate the chains have been converged in all cases. For the sake of brevity, the values of the Geweke's statistic are not reported here. Figure 3 illustrates the trace plot and Auto-Correlation Function (ACF) of the posterior samples obtained for the linear model's parameters of the drought duration attribute under the RCP4.5 scenario as an example. The trace plots reveal no upward and downward trend in simulated samples, which is consistent with the convergence results. The ACF plots also demonstrate that the samples are independent within chains, indicating a good mixing performance of the Markov chain through time. The trace plots obtained

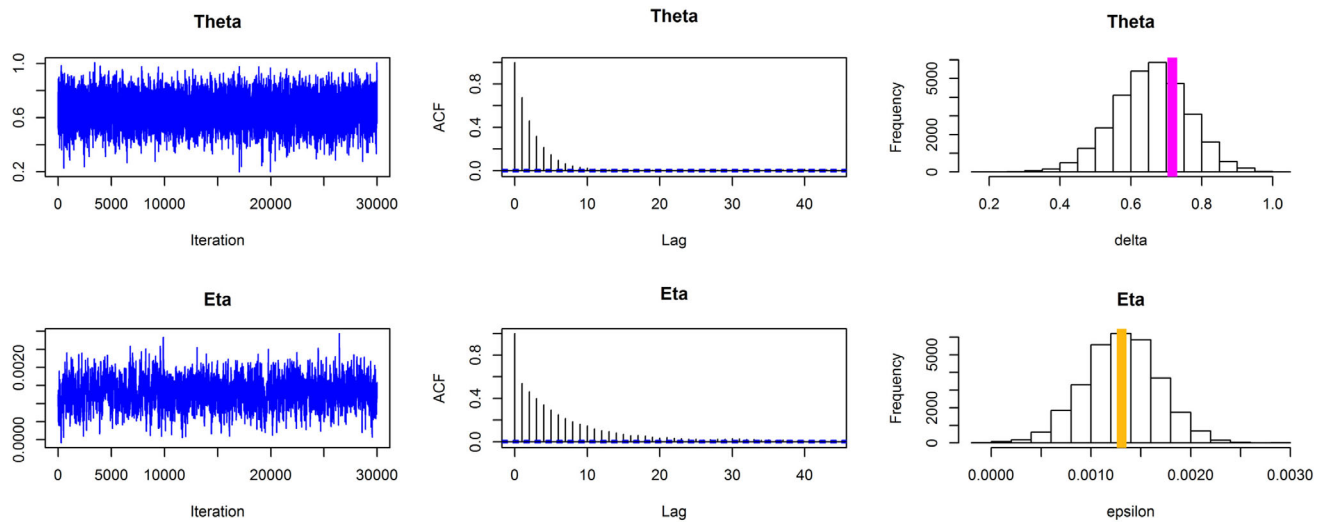


Figure 3. Trace plots for posterior samples obtained using MCMC chains for the parameters of the linear nonstationarity model on drought duration under the RCP4.5 scenario.

for the parameters of the other modes and other attributes also indicate good mixing, but they are not reported here for the sake of saving space.

Having multiple forms of models capturing stationarity and different complex types of nonstationarity, the performance of the DIC measure is examined to select the best Bayesian model for estimation of the time-dependent marginal distributions, interarrival time and copula parameters. After selection of the best Bayesian model, the Bayesian posterior mean is used to produce estimates for the distribution parameters of interest over time that are subsequently used for the time-varying multivariate risk analysis. In the following, the results of the procedure are described for the marginal, the dependence structure of drought severity and duration characteristics, and interarrival time attribute under the three selected climate change scenarios.

#### 4.2.1. RCP2.6 Bayesian Model

The results of the DIC for each drought attribute in different forms of nonstationarity under the scenario RCP2.6 are given in Table 2. In this scenario for the severity attribute, the results of the DIC show that the

**Table 2.** Parameter Estimation and DIC Results of the Different Forms of the Generalized Bayesian Models Under RCP2.6 Scenario

Scenario	Attribute	Statistical Model	Parameters	Posterior Mean	Posterior St.	DIC	
RCP2.6	Severity	<b>M0</b>	$\partial$	1.207	0.109	<b>646.39</b>	
			$\partial$	1.15	0.15	648.02	
		M1	$\rho$	0.001	0.002		
			$\partial$	1.15	0.20		
			$\rho$	0.001	0.012	650.50	
			$\iota$	-1.27	0.0001		
	Duration	<b>M0</b>	$\eta$	1.32	0.11	749.8	
			$\theta$	0.001	0.0003		
		M1	$\eta$	0.733	0.22	743.23	
			$\theta$	0.001	0.0003		
			<b>M2</b>	$\eta$	0.512	0.220	
			$\theta$	0.002	0.0005	<b>742.08</b>	
Interarrival time	<b>M0</b>	$\kappa$	-1.355	4.476			
		$\psi$	1.43	0.08	792.62		
	M1	$\psi$	1.65	0.17	792.29		
		$\omega$	-0.0004	0.0003			
	<b>M2</b>	$\psi$	1.36	0.18			
		$\omega$	0.001	0.0006	<b>786.54</b>		
Copula	<b>M0</b>	$\vartheta$	-1.92	5.91			
		$\xi$	0.620	0.102	-191.44		
		$\nu$	0.105	0.033			
	<b>M1</b>	$\xi$	0.110	0.214	<b>-195.48</b>		
		$\nu$	-0.401	0.521			
		$\nu$	0.386	0.217	-193.9		
	M2	$\xi$	-0.401	0.521			
		$\nu$	0.386	0.217			
		$\chi$	-0.027	0.020			

Bold signifies the best selected statistical model for each attribute.

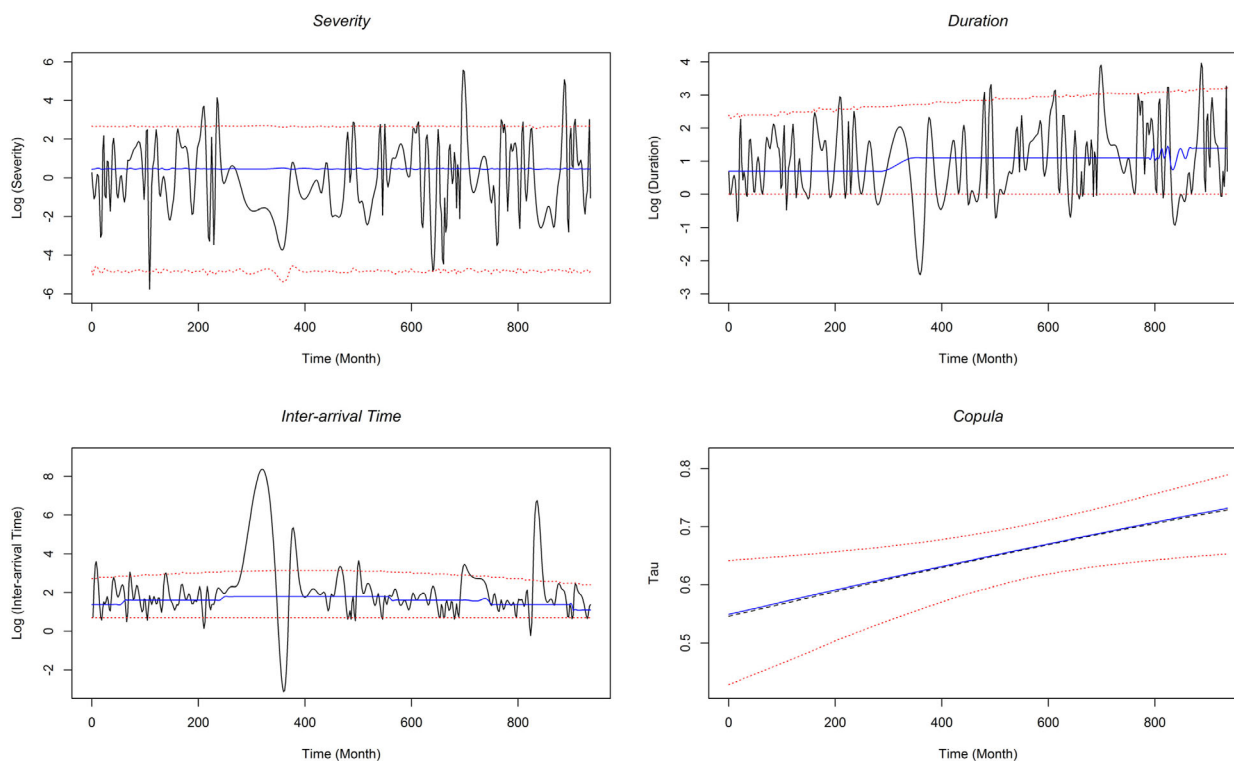


**Figure 4.** Predictive mean (blue-dashed lines), true mean of Kendall's  $\tau_t$ (black-dashed line), 95% Bayesian confidence intervals (red-dotted lines), and drought attribute time series (solid black lines) under forcing scenario RCP2.6.

constant stationary model presents better fit to severity data. Thus, none of the nonstationary models is adequate to describe the behavior of severity characteristic over time.

Unlike the severity, consistent with the trend analysis output, the results of the DIC indicate that the drought duration follows a nonstationary probabilistic time-dependent behavior. Although the DIC values of the linear and the quadratic models are not very different, the quadratic Bayesian model shows the least DIC and it is therefore selected as the best model for estimation of the time-dependent negative binomial distribution. Similar to the duration, the quadratic model is also selected as the best model to describe the probabilistic time-varying behavior of the interarrival time variable in a nonstationary condition.

In terms of the dependency between the severity and duration characteristics (copula variable), the results indicate that a linear nonstationary model provides the best result. Although one of the marginals (duration) exhibits a quadratic nonstationary time-dependent behavior, analogously the DIC results reveal that the linear nonstationary model is required to describe the copula over time. Therefore, it can be concluded that under the RCP2.6 scenario, which is called a peak-decline scenario, the influence of nonstationarity on the marginal distribution (here duration) is larger than the copula dependence measure. The results of the mean and standard deviation of the estimated parameters for each Bayesian model are given in Table 2. Figure 4 illustrates the smoothed log form of drought attribute time series as function of time and the best-fitted time-dependent models.

#### 4.2.2. RCP4.5 Bayesian Model

The results of the time-varying models for the drought attributes under the scenario of RCP4.5 are given in Table 3. For the severity characteristic, the derived DIC values indicate that the constant model is the most adequate model to describe the probabilistic behavior of severity observations.

In terms of the drought duration attribute, the time-varying negative binomial distribution is described in different forms of nonstationarity. The results indicate that the linear model is an adequate model to capture the time-varying rate of drought occurrence over time under this climate change forcing scenario.

**Table 3.** Parameter Estimation and DIC Results of the Different Forms of the Generalized Bayesian Models Under RCP4.5 Scenario

Scenario	Attribute	Statistical Model	Parameters	Posterior Mean	Posterior St.	DIC
RCP4.5	Severity	<b>M0</b>	$\partial$	1.298	0.104	<b>644.21</b>
			M1	$\partial$	1.14	0.16
		M2	$\varrho$	0.003	0.002	
			$\partial$	1.17	0.23	
			$\varrho$	0.001	0.013	647.21
			$\iota$	3.14	0.0001	
	Duration	<b>M0</b>	$\eta$	1.42	0.11	731.94
			<b>M1</b>	$\eta$	0.715	0.211
		M2	$\theta$	0.001	0.0003	
			$\eta$	0.58	0.23	
			$\theta$	0.002	0.0005	722.93
			$\kappa$	-0.976	2.83	
	Interarrival time	M0	$\psi$	1.483	0.089	759.57
			M1	$\psi$	1.756	0.197
		<b>M2</b>	$\omega$	-0.0005	0.0003	
			$\psi$	1.688	0.195	
			$\omega$	-0.0003	0.0004	<b>758.70</b>
			$\vartheta$	1.087	0.166	
	Copula	M0	$\xi$	0.655	0.104	-192.73
			<b>M1</b>	$\xi$	0.046	0.224
		M2	$\nu$	0.129	0.036	
$\xi$			-0.049	0.383		
$\nu$			0.183	0.176	-203.36	
$\chi$			-0.005	0.017		

Bold signifies the best selected statistical model for each attribute.

Quite similar to the low emission scenario (RCP2.6), the results of the DICs indicate the superiority of the quadratic model with respect to the time-varying interarrival time attribute. The results of the predictive posterior mean and the Bayesian predictive intervals are illustrated in Figure 5. Observe that the 95% predictive intervals for the interarrival time attribute are narrow with the selected model, as some of the observations lie outside of the intervals. This seems realistic as around 5% of the observed data should be outside of these predictive intervals.

Similar to the RCP2.6 scenario, the results of the time-varying Gumbel copula show that the linear function fits as the best model to the dependency structure.

#### 4.2.3. RCP8.5 Bayesian Model

The Bayesian modeling under the RCP8.5 is an interesting example demonstrating the importance of using a fully nonstationary-based Bayesian model for all the attributes in a temporal evolution of the climate under a worst-case scenario.

Testing three different Bayesian models with respect to the drought attributes under the current scenario demonstrates that based on the DIC criterion, the quadratic model is the best model describing the time-varying selected distributions for all the attributes (Table 4). The results obtained from the time-varying models are completely consistent with the trend analysis outputs and demonstrate the superiority of nonstationary quadratic-based Bayesian models in capturing a multivariate time-varying environment. Unlike the two previous scenarios, since under the current scenario both the severity and duration attributes exhibit a quadratic nonstationary time-dependent probabilistic behavior, the quadratic generalized Bayesian model proves to be an adequate model in describing the multivariate conditional dynamic copula. Figure 6 illustrates the drought attribute time series and the time-varying fitted Bayesian models under the RCP8.5 scenario.

Overall, the results of the Bayesian modeling demonstrate the complex nonstationary environments under three different climate change scenarios. The results also demonstrate the capability of the proposed methodology in modeling the different types of time-varying nonstationarities in the underlying attributes arising from the complex environments under different radiative forcing scenarios.

#### 4.3. Bayesian Time-Varying Joint Return Period

After selecting the best Bayesian models and constructing time-varying distributions and copula on the drought multiattributes using the MCMC algorithm, the results are employed in creating time-varying joint

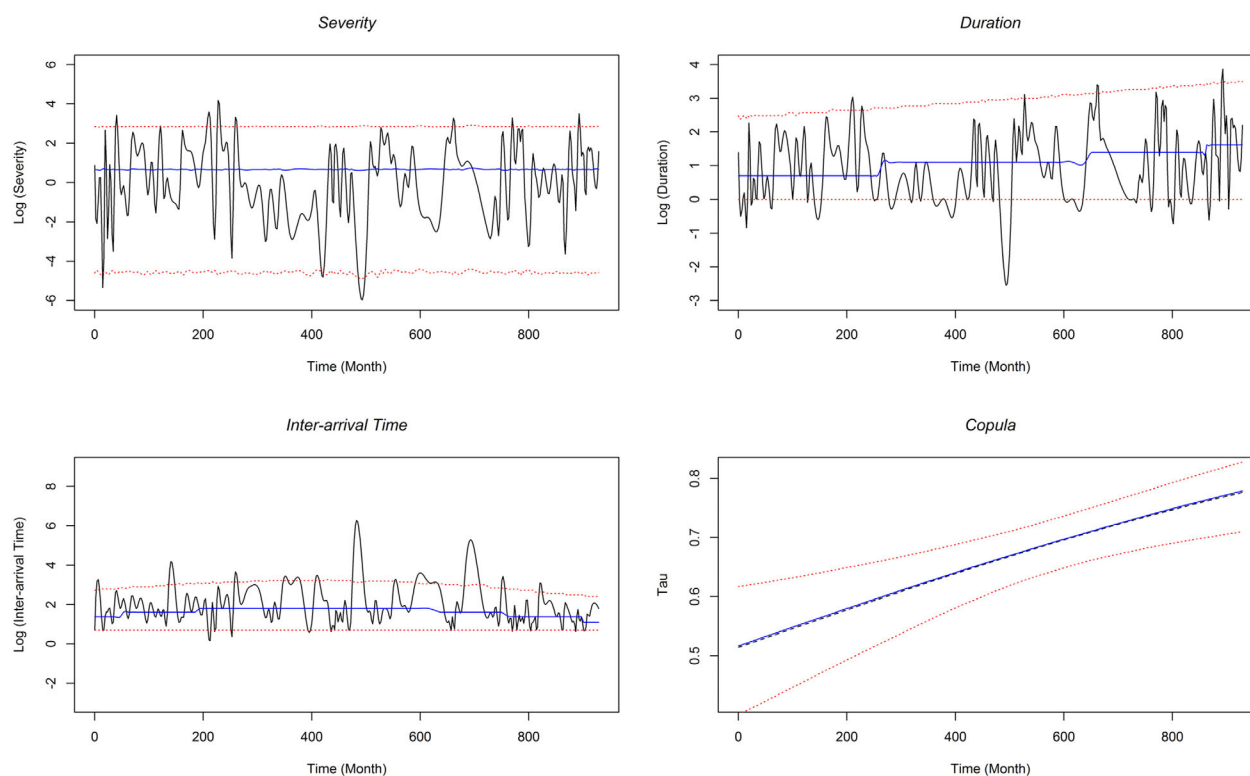


**Figure 5.** Predictive mean (blue-dashed lines), true mean of Kendall's  $\tau_t$ (black-dashed line), 95% Bayesian confidence intervals (red-dotted lines), and drought attribute time series (solid black lines) under forcing scenario RCP4.5.

return period in a multivariate risk framework. The results are given for the three forcing scenarios. In each scenario, as the time-varying joint return period plots cannot be shown over time in a 2-D plot, three time frames from the design's life time period are selected for illustration of the time variation on the time-varying joint return period. The first time frame is year 2015, in which the historical observations till this time are employed for creating time-varying joint return period. The second time slice is 2065, a half century after 2015. Over this time period, the time-varying joint return period is updated as time goes by. The last time frame is the end of the 21st century (year 2100). To show the performance of the proposed time-varying framework, the results of the time-varying nonstationary multivariate risk analysis are also compared with the outputs of the currently used time-independent stationary multivariate framework for the same time slices under the three forcing scenarios.

In following the results of the time-varying nonstationary accompany with the time-independent stationary multivariate risk analysis are given for the low and midrange green-house gas emission scenarios (RCP2.6 and RCP4.5) and the worst-case forcing scenario (RCP8.5), respectively.

#### 4.3.1. Time-Varying Joint Return Period Under RCP2.6 and RCP4.5

To show the time-varying nonstationary multivariate risk, the contours of joint probability for drought severity and duration using the dynamic copula and including the time-varying interarrival time attribute are illustrated in Figure 7a for the three time slices under scenario RCP2.6. The results of the time-independent stationary multivariate risk are also illustrated in Figure 7b for the three time slices under the same scenario. In these plots, historical observations and projected downscaled observations are exhibited separately. A critical return period covering the whole historical drought event is also highlighted as a milestone to better illustrate the flow of time-varying joint return period through time. At the first selected time slice (2015) in the time-varying multivariate framework, the historical drought events are located in the downside of the joint return period plot. This indicates that the majority of drought events occurring in this area have low joint return periods of less than 20 years. By the end of 2065, the majority of drought events are projected to occur with similar characteristics to those of the historical events based on the same framework, whereas some more severe drought events are likely to occur with return period between 20 and 100 years. At the end of the century, as seen in the plot, the number of



**Table 4.** Parameter Estimation and DIC Results of the Different Forms of the Generalized Bayesian Models Under RCP8.5 Scenario

Scenario	Attribute	Statistical Model	Parameters	Posterior Mean	Posterior St.	DIC
RCP8.5	Severity	M0	$\partial$	1.023	0.099	634.49
			$\partial$	0.796	0.172	634.05
		M2	$\varrho$	0.004	0.003	<b>626.53</b>
			$\partial$	1.267	0.222	
			$\varrho$	-0.032	0.013	
			$\iota$	0.0004	0.0001	
	Duration	M0	$\eta$	1.151	0.110	746.35
			$\eta$	0.557	0.213	738.21
		M2	$\theta$	0.001	0.0003	<b>737.39</b>
			$\eta$	0.570	0.207	
			$\theta$	0.0009	0.0003	
			$\kappa$	1.660	2.241	
	Inter-arrival time	M0	$\psi$	1.358	0.090	815.77
			$\psi$	1.688	0.179	813.20
		M2	$\omega$	-0.0006	0.0003	<b>811.48</b>
			$\psi$	1.605	0.180	
			$\omega$	-0.0002	0.0003	
			$\vartheta$	-4.781	1.965	
	Copula	M0	$\xi$	0.572	0.100	-183.84
			$\xi$	0.329	0.219	-186.88
		M2	$\nu$	0.043	0.035	<b>-200.40</b>
$\xi$			0.570	0.416		
$\nu$			-0.980	0.190		
$\chi$			0.013	0.017		

Bold signifies the best selected statistical model for each attribute.

extreme drought events that are more severe and longer (passing the critical return period) will likely be increased under this climate change scenario.

As illustrated in Figure 7a, as time goes by, the time-varying joint contour plots are moving forward (tractable by following the critical RP contour) indicating that the time between drought events is decreasing and

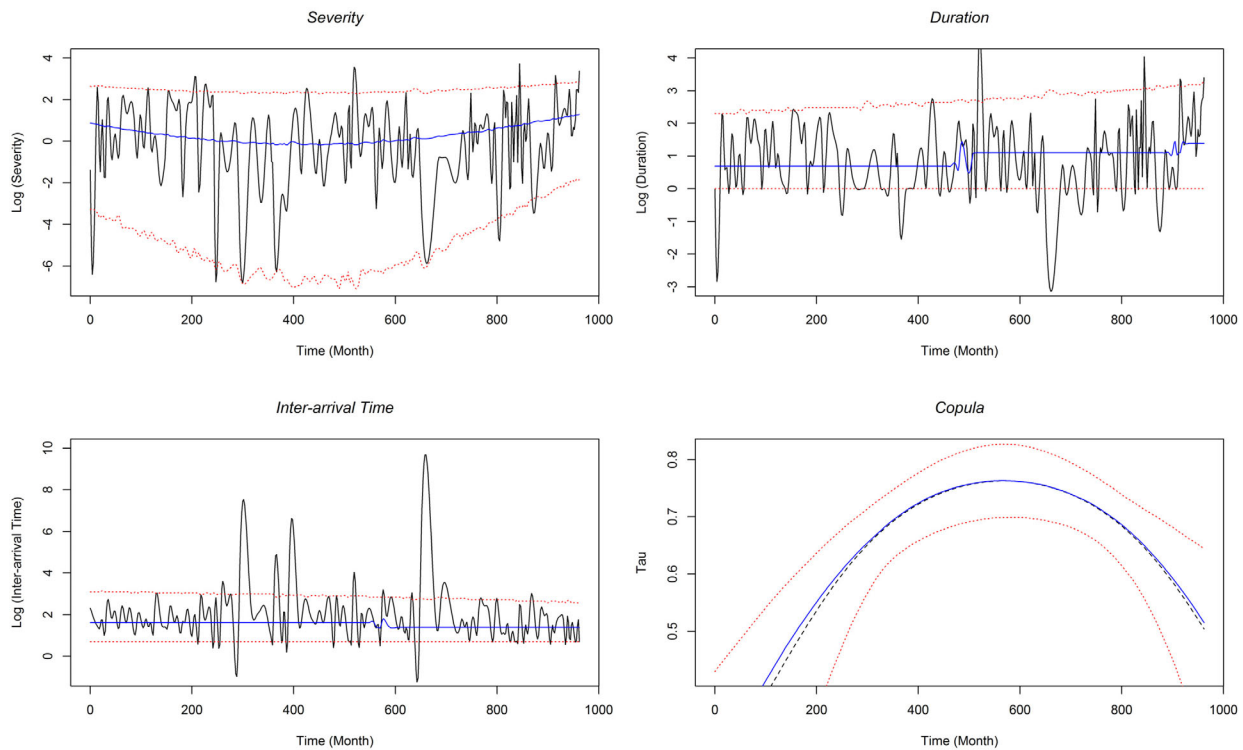


**Figure 6.** Predictive mean (blue solid lines), true mean of Kendall's  $\tau$  (black-dashed line), 95% Bayesian confidence intervals (red-dotted lines), and drought attribute time series (black solid lines) under forcing scenario RCP8.5.

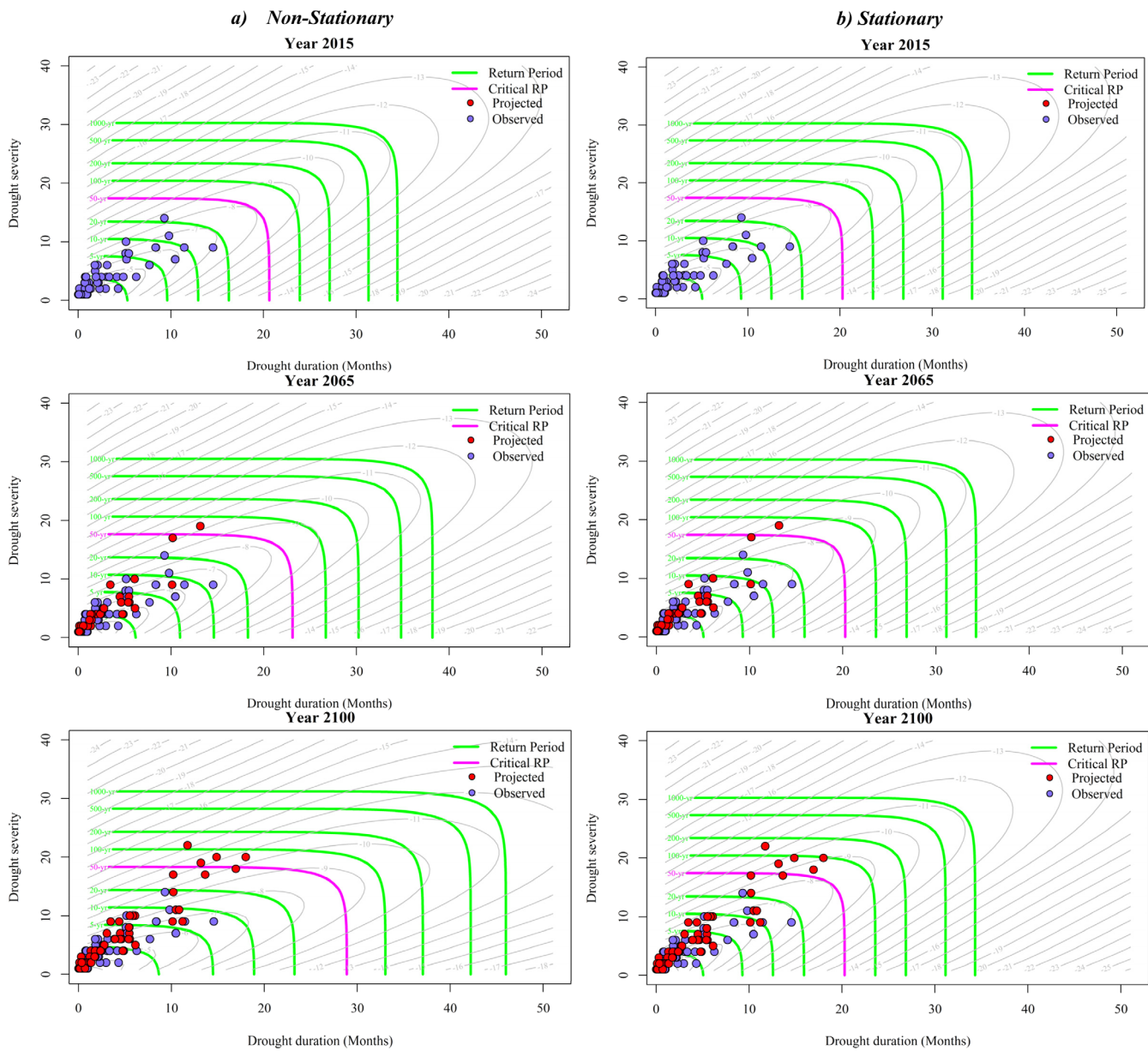


Figure 7. Dynamic joint return period plots at three-selected time frames under scenario RCP2.6.

they are becoming more frequent over design's life period. In contrast, in the time-independent stationary framework illustrated in Figure 7b, the risk of droughts is unchanged over the entire century without any changes in the characteristics of historical and projected droughts.

In Figure 8a, the results of the joint return period are illustrated based on the selected time-varying nonstationary models under the forcing scenario RCP4.5. As exhibited at the first time frame, all drought events occur under return period 10 years. Compared with the same time in the same framework under scenario RCP2.6, the drought events are much more frequent. It should be noted that the drought characteristics are extracted from the synthesized historical and projected precipitation time series. Synthesizing historical precipitation with different projected precipitation time series under different climate change scenarios leads to different SPI time series and subsequently different drought characteristics. That is the reason that the different time-varying joint probability is achieved over the first time period (2015) under the two underlying scenarios, whereas the historical observations are completely similar in the three scenarios. It is likely as time goes on a half century until 2065 under the current scenario, both frequent and rare extreme drought

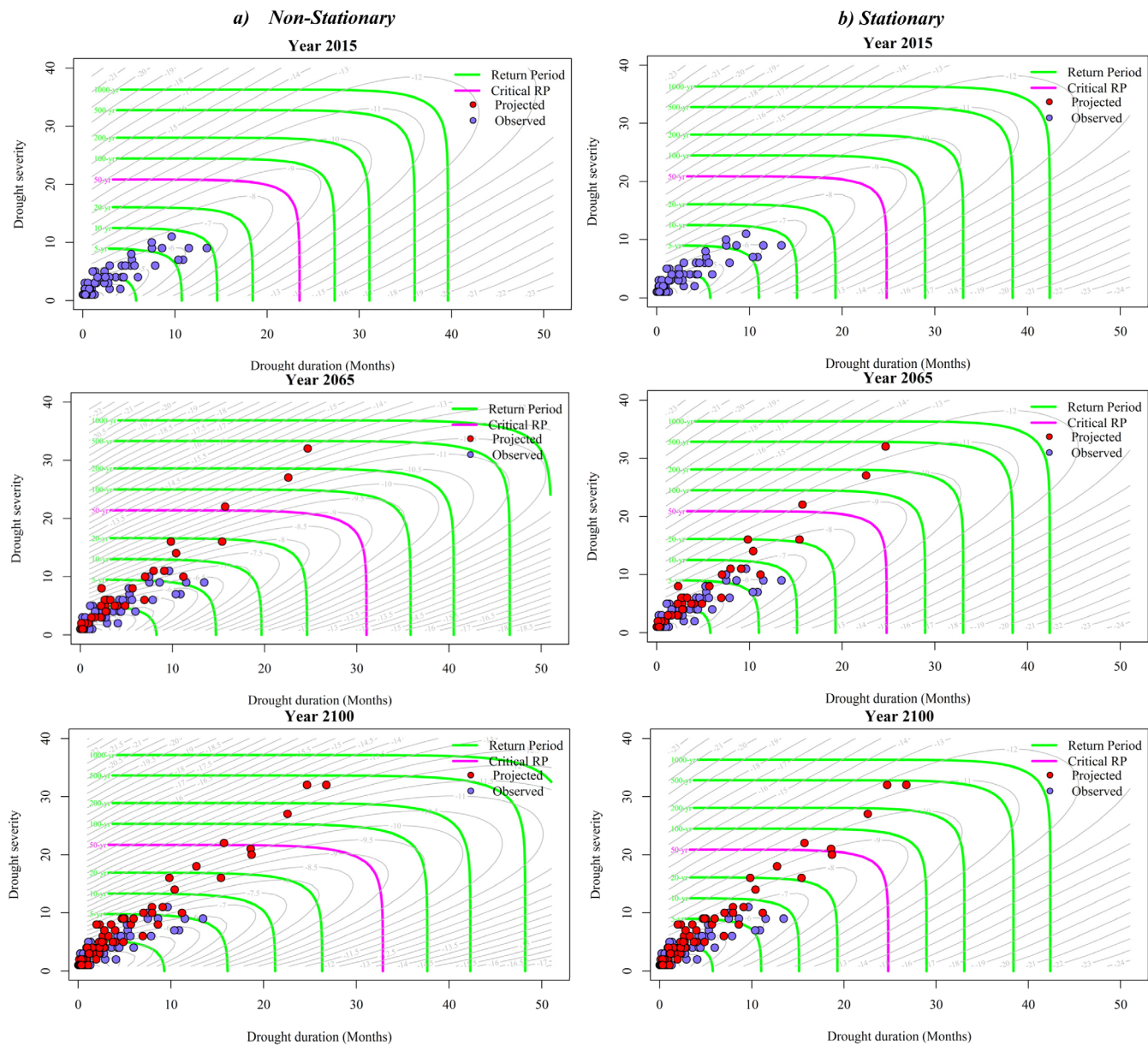


Figure 8. Dynamic joint return period plots at three-selected time frames under scenario RCP4.5.

events (especially rare worst extreme events with return period between 50 and 500 years) will be increased in comparison with the same time period in the previous scenario. Over the last time period, although the number of frequent drought events (under the critical return period) is increased, only one extreme event with return period more than 50 year is projected to occur. In other words, the most extreme severe rare drought events are likely occur over the second time period (2015–2065), which is consistent with the trend of green-house gas emission under RCP4.5 forcing scenario [Taylor et al., 2012]. Looking at the time-varying joint contour plots, the results indicate as time goes by over the design’s life period, as same as the previous scenario, the characteristics of droughts are changed and the expected time between extreme drought events is substantially decreased. Illustrated in Figure 8b, the results of the multivariate risk analysis in the stationary condition, however, indicate that the probabilistic characteristics of droughts will remain unchanged over time using currently used time-independent marginals and copula models.

Comparing each time slice in the two time-varying nonstationary and time-independent stationary risk analyses under scenarios RCP2.6 and RCP4.5, the stationary multivariate framework underestimates the risk

of multivariate drought event occurrences and the drought characteristics over time in comparison with the nonstationary multivariate one. In terms of drought characteristics, as the duration exhibits a nonstationary behavior under these two climate scenarios (statistical models M2 and M1, in Table 2 and 3) than the stationary behavior of severity, a remarkable discrepancy is seen relative to the drought duration than the drought severity in the two frameworks over time.

**4.3.2. Time-Varying Joint Return Period Under RCP8.5**

Modeled by quadratic-based Bayesian functions in terms of all the attributes, the time-varying multivariate risk analysis under this scenario is carried out in a fully nonstationary condition. Figure 9a illustrates the time-varying joint return period plots at the three selected time frames under this scenario. As shown at the first time slice, the historical droughts over the time period until 2015 are having more severe and lengthier duration in comparison with the other two scenarios, so that more events are observed between return period 20 and 50 year. Ignoring the actual nonstationary environment by this time, the multivariate stationary framework, however, overestimates the risk of multivariate drought occurrences and the drought characteristics (shown in Figure 9b). As time progresses, in the second time period, the number of extreme

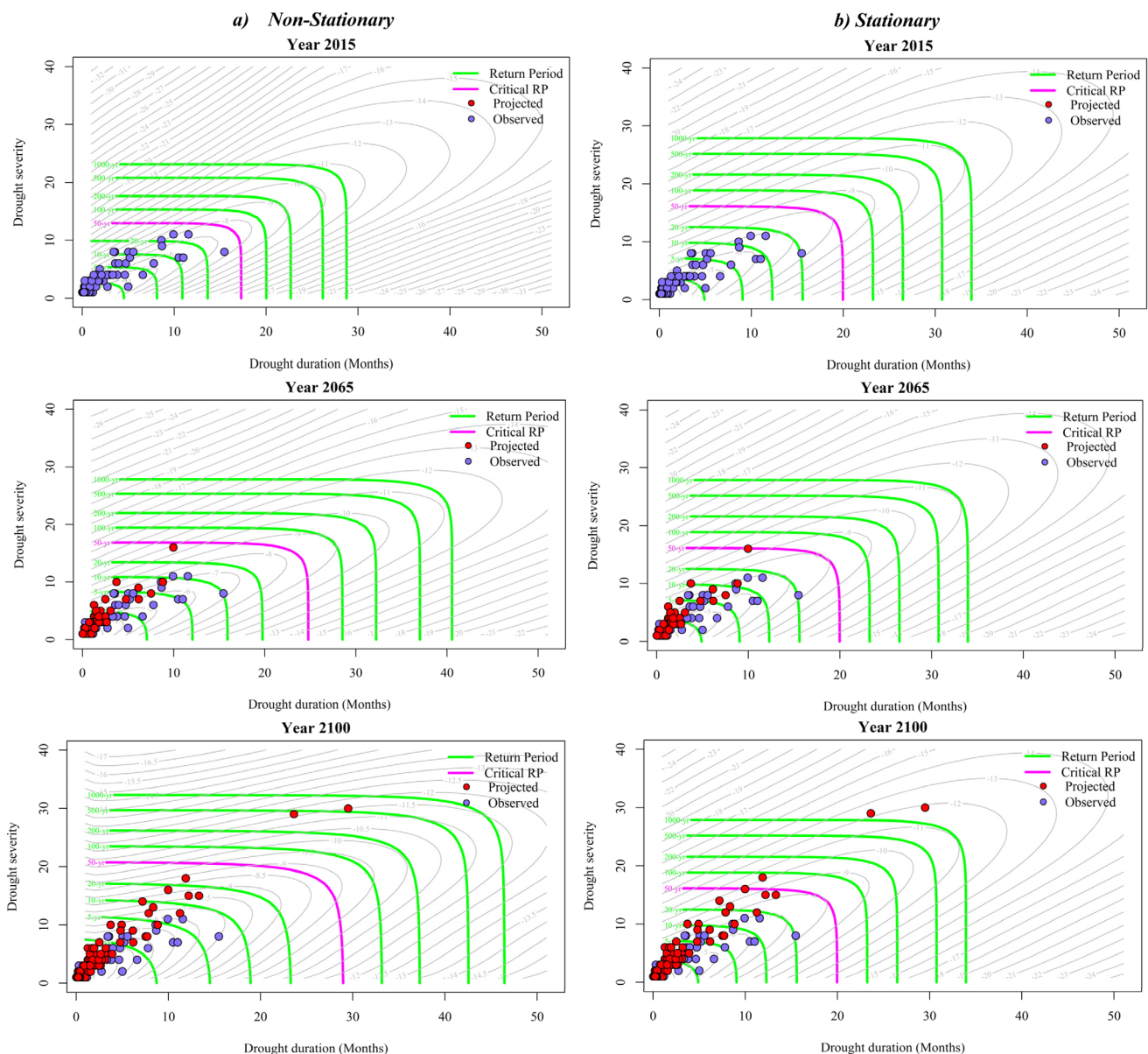


Figure 9. Dynamic joint return period plots at three-selected time frames under scenario RCP8.5.

events is not increased, and the majority of drought events will probably occur with the same characteristics as the historical events based on the multivariate nonstationary risk framework. However, it is interesting that the time between drought events are decreased in comparison with the other two scenarios. For instance, the events between contour plots of 20–50 years, seen in the previous time slice no longer exist over this time period and they have become much more frequent and moved toward the lower joint return periods. That demonstrates that the drought characteristics are changing over time under the impact of the worst-case climate change scenario. In multivariate stationary framework, however, the risk and the nature of droughts are unchanged over time. In comparison with the nonstationary environment, the time-independent stationary assumption underestimates the length and the risk of droughts (especially frequent droughts) by this time slice. Over the last time period, not only the number of much more severe and lengthy droughts will likely be increased under the critical return period, but also two rare extreme events probably occur under this worst forcing scenario based on the time-varying nonstationary risk framework. The return period of these events are between 500 and 1000 years, meaning that they are extreme droughts with large potential damage consequences. However, the currently used multivariate time-independent stationary-based risk analysis shows remarkable discrepancy with the multivariate time-varying nonstationary one so that it underestimates the risk of drought occurrences (for all the frequent and extreme events) and both the drought severity and drought duration. Therefore, the adverse consequences arising from ignoring the nonstationary condition and changing the nature and the risk of droughts in the time-independent stationary multivariate framework under this climate change scenario will seriously threaten various sectors of the Tehran city, especially drinking water sector.

In comparison to the other two scenarios (RCP2.6 and RCP4.5), all the multiattributes (including marginal, copula, and interarrival time) are exhibiting a nonstationary behavior under this scenario. Since the joint return period is also a function of the time-varying multiattributes, as time progresses over the design's life period, the speed of the forward moving of the contour plots is consequently greater than the previous scenarios. That indicates the nature of drought characteristics are severely and fast changed under this worst greenhouse gas emission scenario (Supporting Information S1 and Movie S1).

Overall future dynamic-nature extreme droughts will be compounded with severe and long-time impacts. In addition, cooccurrence of more severe droughts accompany with soaring temperature arising from global warming will increase water demand and the challenge of water resources allocation for various sectors, especially drinking water. As drought characteristics change over time through anthropogenic effects, lessons from the past droughts cannot be applied to the future drought events [AghaKouchak *et al.*, 2015]. Thus, to mitigate adverse consequences, water resources authorities should be prepared for new characterized drought situations in a warmer environment by defining proactive and long-term effective drought management strategies. Infrastructure adaptations, demand management, improving water-conservation technologies, developing an advanced prediction-monitoring system, raising awareness and public perception, and long-term water policy reforms could be some management long-term mitigation strategies.

## 5. Conclusions and Future Work

Climate change is impacting hydrological processes leading to increasing the risk of climate extremes. Accordingly, time-varying nonstationary-based multivariate probabilistic modeling concepts should be developed and adopted for risk-based decision-making in water resources planning and designs.

In the present study, a Bayesian procedure is proposed to perform joint Bayesian inference for a conditional copula model describing dependence between continuous (drought severity) and discrete (drought duration) attributes. The Bayesian inference approach allows estimation of time-varying marginal and copula distribution parameters in a two-stage estimation procedure for mixed complicated situations when one of the marginals is discrete. To capture different types of nonstationarity through time, the Bayesian inference is employed to estimate different formats of the generalized linear model parameters. To make the inference and to estimate the parameters, the Gibbs MCMC sampler is employed to generate sample realizations from the posterior distributions. Moreover, the credibility of the Bayesian predictive intervals are also developed providing information about the precision of the estimates. This study has also improved the concept of the joint return period in multivariate risk studies to a fully time-varying joint return period concept through considering interarrival time as a time-varying attribute.

The proposed approach in the present study offers a number of advantages. One of the main benefits is producing fully likelihood-based inference to model complex time-varying multivariate nonstationary condition arising from climate change. The approach is able to handle modeling any complex hydroclimate extreme phenomena with complicated time-varying dependence structures consisting of mixed attributes (continuous and discrete). It is also flexible for modeling mixtures of stationary and nonstationary conditions for multiattributes. The study also demonstrates that the risk of multidimensional extreme climate processes becomes time-varying under the impact of climate change. Accordingly, to mitigate adverse consequences arising from these new characterized natural hazards, the associated authorities should keep updating long-term proactive strategies based on anomalies of dynamic anthropogenically forced environments.

The new proposed insight of dynamic joint Bayesian inference copula will replace the time-varying multivariate concept of risk analysis with the currently used time-independent stationary multivariate risk in climate change studies. Thus future work can focus on developing the same concept for different copula families and compare their performances for selecting the best dynamic copula. Using simultaneous estimation of both marginal and copula distributions' parameters in contrast with the two-stage procedure may lead to better understanding of the parameter dependences and also result in better performance of model selection criteria.

#### Acknowledgments

We thank the associate editor and three anonymous reviewers whose suggestions helped improve the paper. We acknowledge the CMIP5 climate coupled modelling groups, for producing and making their model outputs available, the U.S. Department of Energy's Program for Climate Model Diagnosis and Intercomparison (PCMDI), which provides coordinating support and led development of software infrastructure in partnership with the Global Organization for Earth System Science Portals. The CMIP5 model outputs used in the present study are available from [http://cmip-pcmdi.llnl.gov/cmip5/data\\_portal.html](http://cmip-pcmdi.llnl.gov/cmip5/data_portal.html). We also thank the Iran Meteorological Organization (IRIMO) for providing rainfall data recorded at the Tehran synoptic station. Funding support was provided by the Natural Sciences and Engineering Research Council (NSERC) of Canada.

#### References

- AghaKouchak, A., D. Easterling, K. Hsu, S. Schubert, and S. Sorooshian (2012), *Extremes in a Changing Climate: Detection, Analysis and Uncertainty*, Springer, N. Y.
- AghaKouchak, A., D. Feldman, M. Hoerling, T. Huxman, and J. Lund (2015), Recognize Anthropogenic Drought, *Nature*, 524(7566), 409–411.
- Ausin, M. C., and H. F. Lopes (2010), Time-varying joint distribution through copulas, *Comput. Stat. Data Anal.*, 54(11), 2383–2399.
- Bayazit, M. (2015), Nonstationarity of hydrological records and recent trends in trend analysis: A state-of-the-art review, *Environ. Processes*, 2(3), 527–542.
- Bender, J., T. Wahl, and J. Jensen (2014), Multivariate design in the presence of non-stationarity, *J. Hydrol.*, 514, 123–130.
- Borgomeo, E., J. W. Hall, F. Fung, G. Watts, K. Colquhoun, and C. Lambert (2014), Risk-based water resources planning: Incorporating probabilistic nonstationary climate uncertainties, *Water Resour. Res.*, 50, 6850–6873, doi:10.1002/2014WR015558.
- Chebana, F., and T. B. Ouarda (2011), Multivariate quantiles in hydrological frequency analysis, *Environmetrics*, 22(1), 63–78.
- Chebana, F., T. B. Ouarda, and T. C. Duong (2013), Testing for multivariate trends in hydrologic frequency analysis, *J. Hydrol.*, 486, 519–530.
- Cheng, L., and A. AghaKouchak (2014), Nonstationary precipitation intensity-duration-frequency curves for infrastructure design in a changing climate, *Sci. Rep.*, 4, 7093 pp.
- Corbella, S., and D. D. Stretch (2013), Simulating a multivariate sea storm using Archimedean copulas, *Coastal Eng.*, 76, 68–78.
- Creal, D. D., and R. S. Tsay (2015), High-dimensional dynamic stochastic copula models, *J. Econ.*, 189(2), 335–345.
- Cunderlik, J. M., V. Jourdain, T. B. Ouarda, and B. Bobée (2007), Local non-stationary flood-duration-frequency modelling, *Can. Water Resour. J.*, 32(1), 43–58.
- De Michele, C., and G. Salvadori (2003), A generalized Pareto intensity-duration model of storm rainfall exploiting 2-copulas, *J. Geophys. Res.*, 108(D2), 4067, doi:10.1029/2002JD002534.
- De Michele, C., G. Salvadori, R. Vezzoli, and S. Pecora (2013), Multivariate assessment of droughts: Frequency analysis and dynamic return period, *Water Resour. Res.*, 49, 6985–6994, doi:10.1002/wrcr.20551.
- DeChant, C. M., and H. Moradkhani (2015), On the assessment of reliability in probabilistic hydrometeorological event forecasting, *Water Resour. Res.*, 51, 3867–3883, doi:10.1002/2014WR016617.
- Dellaportas, P., and A. F. Smith (1993), Bayesian inference for generalized linear and proportional hazards models via Gibbs sampling, *Appl. Stat.*, 42(3), 443–459.
- Du, T., L. Xiong, C.-Y. Xu, C. J. Gippel, S. Guo, and P. Liu (2015), Return period and risk analysis of nonstationary low-flow series under climate change, *J. Hydrol.*, 527, 234–250.
- El Adlouni, S., and T. B. M. J. Ouarda (2009), Joint Bayesian model selection and parameter estimation of the generalized extreme value model with covariates using birth-death Markov chain Monte Carlo, *Water Resour. Res.*, 45, W06403, doi:10.1029/2007WR006427.
- El Adlouni, S., T. Ouarda, X. Zhang, R. Roy, and B. Bobée (2007), Generalized maximum likelihood estimators for the nonstationary generalized extreme value model, *Water Resour. Res.*, 43, W03410, doi:10.1029/2005WR004545.
- Galloway, G. E. (2011), If stationarity is dead, What do we do now?1, *J. Am. Water Resour. Assoc.*, 47(3), 563–570.
- Geweke, J. (1991), *Evaluating the Accuracy of Sampling-Based Approaches to the Calculation of Posterior Moments*, Fe. Reserve Bank of Minneapolis, Res. Dep. Minneapolis, Minn.
- Gräler, B., M. van den Berg, S. Vandenbergh, A. Petroselli, S. Grimaldi, B. D. Baets, and N. Verhoest (2013), Multivariate return periods in hydrology: A critical and practical review focusing on synthetic design hydrograph estimation, *Hydrol. Earth Syst. Sci.*, 17(4), 1281–1296.
- Halwatura, D., A. Lechner, and S. Arnold (2015), Drought severity–duration–frequency curves: A foundation for risk assessment and planning tool for ecosystem establishment in post-mining landscapes, *Hydrol. Earth Syst. Sci.*, 19(2), 1069–1091.
- Hao, Z., and V. Singh (2012), Entropy-copula method for single-site monthly streamflow simulation, *Water Resour. Res.*, 48, W06604, doi:10.1029/2011WR011419.
- IPCC (2014), Summary for policymakers, in *Climate Change 2014, Synthesis Report*, edited by The Core Writing Team, R. K. Pachauri, and L. Meyer, pp. 6–15. Geneva. [Available at [http://www.ipcc.ch/pdf/assessment-report/ar5/syr/SYR\\_AR5\\_SPMcorr2.pdf](http://www.ipcc.ch/pdf/assessment-report/ar5/syr/SYR_AR5_SPMcorr2.pdf).]
- Jammazi, R., A. K. Tiwari, R. Ferrer, and P. Moya (2015), Time-varying dependence between stock and government bond returns: International evidence with dynamic copulas, *North Am. J. Econ. Finance*, 33, 74–93.
- Janga Reddy, M., and P. Ganguli (2012), Application of copulas for derivation of drought severity–duration–frequency curves, *Hydrol. Processes*, 26(11), 1672–1685.

- Jiang, C., L. Xiong, C. Y. Xu, and S. Guo (2015), Bivariate frequency analysis of nonstationary low-flow series based on the time-varying copula, *Hydrol. Processes*, 29(6), 1521–1534.
- Katz, R. W., M. B. Parlange, and P. Naveau (2002), Statistics of extremes in hydrology, *Adv. Water Resour.*, 25(8–12), 1287–1304.
- Khaliq, M. N., T. B. M. J. Ouarda, J. C. Ondo, P. Gachon, and B. Bobée (2006), Frequency analysis of a sequence of dependent and/or nonstationary hydro-meteorological observations: A review, *J. Hydrol.*, 329(3–4), 534–552.
- Leclerc, M., and T. B. M. J. Ouarda (2007), Non-stationary regional flood frequency analysis at ungauged sites, *J. Hydrol.*, 343(3–4), 254–265.
- Lee, T., R. Modarres, and T. Ouarda (2013), Data-based analysis of bivariate copula tail dependence for drought duration and severity, *Hydrol. Processes*, 27(10), 1454–1463.
- Lloyd-Hughes, B., and M. A. Saunders (2002), A drought climatology for Europe, *Int. J. Climatol.*, 22(13), 1571–1592.
- Madadgar, S., and H. Moradkhani (2013), Drought analysis under climate change using copula, *J. Hydrol. Eng.*, 18(7), 746–759.
- Madadgar, S., and H. Moradkhani (2014), Improved Bayesian multimodeling: Integration of copulas and Bayesian model averaging, *Water Resour. Res.*, 50, 9586–9603, doi:10.1002/2014WR015965.
- McKee, T. B., N. J. Doesken, and J. Kleist (1993), The relationship of drought frequency and duration to time scales, paper presented at Proceedings of the 8th Conference on Applied Climatology, Am. Meteorol. Soc., Boston, Mass.
- Milly, P. C. D., J. Betancourt, M. Falkenmark, R. M. Hirsch, Z. W. Kundzewicz, D. P. Lettenmaier, and R. J. Stouffer (2008), Stationarity is dead: Whither water management?, *Science*, 319, 573–574.
- Milly, P. C. D., J. Betancourt, M. Falkenmark, R. M. Hirsch, Z. W. Kundzewicz, D. P. Lettenmaier, R. J. Stouffer, M. D. Dettinger, and V. Krysanova (2015), On critiques of “Stationarity is dead: Whither water management?,” *Water Resour. Res.*, 51, 7785–7789, doi:10.1002/2015WR017408.
- Mishra, A. K., and V. P. Singh (2010), A review of drought concepts, *J. Hydrol.*, 391(1), 202–216.
- Mishra, A. K., and V. P. Singh (2011), Drought modeling: A review, *J. Hydrol.*, 403(1), 157–175.
- Nelsen, R. B. (2007), *An introduction to copulas*, Springer, N. Y.
- Ouarda, T., and S. El-Adlouni (2011), Bayesian nonstationary frequency analysis of hydrological variables, *J. Am. Water Resour. Assoc.*, 47(3), 496–505.
- Patton, A. J. (2006), Modelling asymmetric exchange rate dependence\*, *Int. Econ. Rev.*, 47(2), 527–556.
- Read, L. K., and R. M. Vogel (2015), Reliability, return periods, and risk under nonstationarity, *Water Resour. Res.*, 51, 6381–6398, doi:10.1002/2015WR017089.
- Requena, A., L. Mediero Orduña, and L. Garrote de Marcos (2013), A bivariate return period based on copulas for hydrologic dam design: Accounting for reservoir routing in risk estimation, *Hydrol. Earth Syst. Sci.*, 17(8), 3023–3038.
- Rootzén, H., and R. W. Katz (2013), Design life level: Quantifying risk in a changing climate, *Water Resour. Res.*, 49, 5964–5972, doi:10.1002/wrcr.20425.
- Rosner, A., R. M. Vogel, and P. H. Kirshen (2014), A risk-based approach to flood management decisions in a nonstationary world, *Water Resour. Res.*, 50, 1928–1942, doi:10.1002/2013WR014561.
- Sadri, S., and D. H. Burn (2012), Copula-based pooled frequency analysis of droughts in the Canadian Prairies, *J. Hydrol. Eng.*, 19(2), 277–289.
- Salas, J. D., and J. Obeysekera (2013), Revisiting the concepts of return period and risk for nonstationary hydrologic extreme events, *J. Hydrol. Eng.*, 19(3), 554–568.
- Salvadori, G., C. De Michele, N. T. Kottegoda, and R. Rosso (2007), *Extremes in Nature: An Approach Using Copulas*, Springer, Dordrecht, Netherlands.
- Santhosh, D., and V. Srinivas (2013), Bivariate frequency analysis of floods using a diffusion based kernel density estimator, *Water Resour. Res.*, 49, 8328–8343, doi:10.1002/2011WR010777.
- Sarhadi, A., H. D. Burn, F. Johnson, R. Mehrotra, and A. Sharma (2015), Water resources climate change projections using supervised nonlinear and multivariate soft computing techniques, *J. Hydrol.*, 536, 119–132.
- Scoccimarro, E., S. Gualdi, A. Bellucci, M. Zampieri, and A. Navarra (2013), Heavy precipitation events in a warmer climate: Results from CMIP5 models, *J. Clim.*, 26(20), 7902–7911.
- Shiau, J.-T. (2006), Fitting drought duration and severity with two-dimensional copulas, *Water Resour. Manage.*, 20(5), 795–815.
- Shiau, J.-T., and R. Modarres (2009), Copula-based drought severity-duration-frequency analysis in Iran, *Meteorol. Appl.*, 16(4), 481–489.
- Sklar, M. (1959), *Fonctions de Répartition à n Dimensions et Leurs Marges*, 8 pp, Univ. Paris, Paris.
- Smith, M. S. (2013), Bayesian approaches to copula modelling, in *Hierarchical Models and MCMC: A Tribute to Adrian Smith*, *Bayesian Statistics*, edited by P. Damien et al., pp. 395–402, Oxford Univ. Press, Oxford, U. K.
- Song, S., and V. P. Singh (2010), Frequency analysis of droughts using the Plackett copula and parameter estimation by genetic algorithm, *Stoch. Environ. Res. Risk Assess.*, 24(5), 783–805.
- Spiegelhalter, D. J., N. G. Best, B. P. Carlin, and A. Van Der Linde (2002), Bayesian measures of model complexity and fit, *J. R. Stat. Soc. Ser. B*, 64(4), 583–639.
- Tallaksen, L. M., and H. A. van Lanen (2004), *Hydrological Drought: Processes and Estimation Methods for Streamflow and Groundwater*, Elsevier, Amsterdam, Netherlands.
- Taylor, K. E., R. J. Stouffer, and G. A. Meehl (2012), An overview of CMIP5 and the experiment design, *Bull. Am. Meteorol. Soc.*, 93(4), 485–498.
- Vogel, R. M., C. Yaoundi, and M. Walter (2011), Nonstationarity: Flood magnification and recurrence reduction factors in the United States 1, *J. Am. Water Resour. Assoc.*, 47(3), 464–474.
- Wahl, T., S. Jain, J. Bender, S. D. Meyers, and M. E. Luther (2015), Increasing risk of compound flooding from storm surge and rainfall for major US cities, *Nat. Clim. Change*, 5(12), 1093–1097.
- Westra, S., M. Thyer, M. Leonard, D. Kavetski, and M. Lambert (2014), A strategy for diagnosing and interpreting hydrological model nonstationarity, *Water Resour. Res.*, 50, 5090–5113, doi:10.1002/2013WR014719.
- Wilhite, D. A. (2000), *Drought as a Natural Hazard: Concepts and Definitions*, chap. 18, pp. 245–255, Routledge, London, U. K.